RESEARCH ARTICLE

THE FASEB JOURNAL

Calreticulin exploits TGF-β for extracellular matrix induction engineering a tissue regenerative process

Unnati M. Pandya[1] | Miguel A. Manzanares[1] | Ana Tellechea[1] | Chinaza Egbuta[1] | Julien Daubriac[1] | Couger Jimenez-Jaramillo[1] | Fares Samra[1] | Alexa Fredston-Hermann[1] | Khalil Saadipour[1] | Leslie I. Gold[1,2]

[1]Division of Translational Medicine, Department of Medicine, New York University School of Medicine-Langone Health, New York, NY, USA

[2]Pathology Department, New York University School of Medicine-Langone Health, New York, NY, USA

Correspondence
Leslie I. Gold, Division of Translational Medicine, Department of Medicine, New York University School of Medicine-Langone Health, 550 First Avenue, MSB-258, New York, NY 10016, USA.
Email: leslie.gold@nyumc.org

Funding information
Calregen, Inc, Grant/Award Number: NA; Tissue Regeneration Sciences, Inc, Grant/Award Number: NA

Abstract

Topical application of extracellular calreticulin (eCRT), an ER chaperone protein, in animal models enhances wound healing and induces tissue regeneration evidenced by epidermal appendage neogenesis and lack of scarring. In addition to chemoattraction of cells critical to the wound healing process, eCRT induces abundant neo-dermal extracellular matrix (ECM) formation by 3 days post-wounding. The purpose of this study was to determine the mechanisms involved in eCRT induction of ECM. In vitro, eCRT strongly induces collagen I, fibronectin, elastin, α-smooth muscle actin in human adult dermal (HDFs) and neonatal fibroblasts (HFFs) mainly via TGF-β canonical signaling and Smad2/3 activation; RAP, an inhibitor of LRP1 blocked eCRT ECM induction. Conversely, eCRT induction of α5 and β1 integrins was not mediated by TGF-β signaling nor inhibited by RAP. Whereas eCRT strongly induces ECM and integrin α5 proteins in K41 wild-type mouse embryo fibroblasts (MEFs), CRT null MEFs were unresponsive. The data show that eCRT induces the synthesis and release of TGF-β3 first via LRP1 or other receptor signaling and later induces ECM proteins via LRP1 signaling subsequently initiating TGF-β receptor signaling for intracellular CRT (iCRT)-dependent induction of TGF-β1 and ECM proteins. In addition, TGF-β1 induces 2-3-fold higher level of ECM proteins than eCRT. Whereas eCRT and iCRT converge for ECM induction, we propose that eCRT attenuates TGF-β-mediated fibrosis/scarring to achieve tissue regeneration.

1 | INTRODUCTION

Calreticulin (CRT) is a 46 kDa highly conserved endoplasmic reticulum (ER) chaperone protein that identifies N-linked glycoproteins and ensures proper protein conformation and prevention of protein aggregation.[1-3] In addition, CRT regulates Ca+ homeostasis between the ER and cytoplasm and is involved in cellular Ca-dependent signaling functions.[1-6] CRT regulates cellular responses to stress and in concert with other ER chaperone proteins, identifies mis-folded proteins for proteasome-mediated destruction outside the ER. In addition, CRT exists in the cytoplasm, cell surface, extracellular space, and plasma and as a multicompartmental protein regulates a wide array of intracellular and extracellular responses important in physiological and pathological responses. Pathological responses include the unfolded protein response (UPR) and fibrosis.[3,7-9] Examples of physiological responses are key roles for CRT in the innate and adaptive immune responses,[3,10-13] namely immunogenic cell death (ICD)[14-20] and as we have previously shown, in wound healing putatively via outside-in receptor signaling.[21-24]

We discovered that topically applied CRT enhances the rate and quality of wound healing in a porcine model of cutaneous injury, which is the closest animal model exemplary of human healing. A consequence of type I and type II diabetes mellitus is chronic nonhealing wounds.[25,26] There are 23 million diabetics in the United States and 347 million worldwide[25,27-30]; 15%-20% will develop chronic plantar neuropathic or neuroischemic wounds with a high percent culminating in amputation incurring a 50% death rate. Using the leptin receptor null (lpr-/lpr-) mouse as a model for diabetes and poor wound healing, we further showed that CRT healed full-thickness excisional wounds by a tissue regenerative process characterized by neogenesis of epidermal appendages, including pigmented hair, and lack of scarring.[22] Extensive in vitro studies revealed that CRT heals wounds by multiple and diverse mechanisms that specifically correct the cellular and molecular pathologies associated with diabetic wounds including lack of recruitment of cells into the wound bed, defective cell proliferation, and a paucity of granulation tissue to reconstruct the wound defect.[22-24]

Notably, CRT functions in all the three phases of wound healing: the inflammatory, proliferative, and remodeling stages. CRT has been shown to be involved in initial blood clotting to form the eschar,[2,31] and the inflammatory phase through chemotaxis of neutrophils and macrophages that release cytokines to start the repair process.[27,32,33] Specifically, in vitro studies using human fibroblasts, keratinocytes, and macrophages show that CRT induces concentration-dependent migration of these cells, proliferation of keratinocytes and fibroblasts, and activates macrophages.[22,23,34-36] CRT on the surface of dead cells provides the "eat me" signal for macrophage lineages,[34,35] a function important for wound debridement. CRT induces abundant granulation tissue (neodermis) during the inflammatory phase that continues through the remodeling maturation phase until wound closure.

The cytokine Transforming growth factor-β (TGF-β) is a key protein responsible for the fibrotic response in nearly every organ in which pathologies such as nephropathies and lung disease culminate in severe fibrosis causing loss of organ function.[5,9,37-42] Similarly, cutaneous wound remodeling is a dynamic process that usually leads to fibrosis/scarring involving TGF-β signaling with downstream focal adhesion kinase (FAK) activation and/or increasing Connective Tissue Growth Factor (CCN2).[43,44] The three mammalian isoforms of TGF-β share 67%-80% amino acid homology and signal through two major receptors, TGF-β RII (TβRII) and TGF-βRI (TβRI).[45,46] Extracellular matrix induction characterizing the fibrotic response occurs mainly through TGF-β canonical signaling involving the binding of TGF-β ligand to TβRII, autophosphorylation and subsequent phosphorylation and dimerization with TβRI, which phosphorylates Smad2/3 transcription factors for downstream target gene activation; PI3K, ERK, and p38MAPK are also intermediate signaling mediators that respond to TGF-β.[7] In addition to canonical TGF-β signaling, the diverse functions of TGF-β involve signaling via a variety of co-receptors, accessory proteins, and responses, which are cell-type and context-dependent.[46-48]

Intracellular CRT (iCRT) was shown to regulate fibrillar collagen expression, secretion, and processing in mouse embryo fibroblasts (MEFs).[6] CRT null MEFs, which are embryonically lethal at 12.5 p.c., have reduced collagen I and III transcripts and cannot process collagen type I for fibrillar collagen deposition into matrix, in part due to a decrease in fibronectin matrix scaffold formation. Considering the role for iCRT in collagen and fibronectin synthesis and deposition into matrix, it is not surprising that TGF-β stimulation of collagen type I and fibronectin were found to require iCRT.[5] Since Smad2/3 activation by TGF-β was retained in CRT$^{-/-}$ cells with decreased collagen and fibronectin (ECM) synthesis, the TGF-β canonical signaling pathway for collagen and fibronectin induction remained intact implicating the requirement for iCRT downstream from TGF-β signaling as the defect in ECM protein synthesis. Moreover, greater expression of collagen and fibronectin was shown in transgenic fibroblasts with increased expression of CRT and interestingly,

TGF-β increases iCRT in human kidney proximal tubule cells suggesting feedback regulatory mechanisms between these two proteins.[49]

As poor formation of granulation tissue is a significant problem of chronic nonhealing wounds, such as diabetic foot ulcers (DFUs), the overarching goal of the current study was to determine the mechanism(s) involved in CRT induction of post-wounding granulation tissue formation (neodermis) for a deeper understanding of potential cellular and molecular targets to improve the serious unmet need of chronic wounds. Moreover, as both TGF-β and exogenous (eCRT) similarly function in ECM induction and CRT -/- mice revealed the requirement for iCRT in the TGF-β-mediated ECM response, the current study was designed to determine whether the induction of ECM proteins by eCRT are mediated by TGF-β signaling requiring iCRT. We show collagen type I, fibronectin and elastin are markedly increased ECM components of the granulation tissue of eCRT-treated diabetic mouse wounds compared to buffer-treated controls. In vitro, eCRT induced collagen type I, fibronectin, elastin, and smooth muscle actin (α-SMA), as well as α5 and β1 integrins in human adult and neonatal dermal fibroblasts. A serine/threonine kinase inhibitor of TβRI signaling, SD208, mainly blocked CRT-mediated induction of ECM proteins and α-SMA, and Smad2/3 activation implicating a strong involvement of CRT-mediated ECM and α-SMA induction on TGF-β release and subsequent TGF-β canonical receptor signaling. The data suggest that eCRT induces the synthesis and release of TGF-β3 in part via LRP1 signaling subsequently, initiating TGF-β autocrine and/or paracrine signaling for TGF-β1, ECM, and α-SMA protein synthesis requiring iCRT. The increased expression of Integrin α5 by eCRT does not involve LRP1 or canonical TGF-β signaling but requires iCRT. On a molar basis, TGF-β1 induces 1.7-3.5-fold higher levels of ECM proteins than eCRT suggesting that whereas ECM induction by eCRT is mediated by TGF-β, which causes fibrosis/scarring, CRT attenuates the TGF-β response by directing a tissue regenerative program.

2 | MATERIALS AND METHODS

2.1 | Reagents

Recombinant human calreticulin (CRT) was expressed by *E coli* (TOP10), purified by Intas Biopharmaceuticals (Ahmedabad, India), as described[50] and stored in buffer containing 10 mM Tris and 3.0 mM calcium, pH 7.0. Recombinant human TGF-β1 was purchased from R&D systems (catalog #100-B-001, Minneapolis, MN). The serine/threonine TGF-β receptor I (TβRI) kinase inhibitor, SD208, was purchased from Tocris Bioscience (catalog #3269, Minneapolis, MN). Low endotoxin containing recombinant

LRP-1 Receptor associated protein (RAP) was obtained from Molecular Innovations (catalog #RAP-LE, Novi, MI). Cytochalasin D was purchased from Gibco, Thermo Fisher Scientific (#PHZ1063, Waltham, MA).

2.2 | Diabetic mouse model of wound healing and treatments

Tissues from CRT-treated wounds from the murine model of diabetic wound healing, as described[22] were used to determine the levels of ECM proteins by immunohistochemistry and elastin staining. Briefly, 10-12 weeks old female db/db leptin receptor-deficient mice (BKS.Cg-*Dock7^m* +/+ *Lepr^{db}*/J, Jackson Laboratories, Bar Harbor, ME) were anesthetized and two circular 6.0-mm full-thickness excisional wounds were created on the shaved and sterilized dorsum.[22] A 12-mm diameter and 0.5-mm thick silicone splint (Grace Bio-Laboratories, Bend, OR) was placed around the wound to prevent wound contraction thereby simulating human healing.[51] The wounds were treated with 5.0 mg/mL CRT (10 μL) in Tris-saline buffer (10 mM Tris, 150 M NaCl, 3 M CaCl, pH 7.0) or with buffer alone for the first 4 days post-injury. Immediately after treatment, the wounds were covered with an occlusive dressing (Tegaderm, 3M, St Paul, MN). The mice were euthanized and the wound tissue excised at days 3, 7, 10, 14, and 28 (n = 6/group) post-injury for histological and immunohistochemical analysis.

2.3 | Histological and immunohistochemical analysis

Wound tissue was fixed in 10% of formalin overnight, embedded in paraffin, and 5-μm tissue sections were deparaffinized, hydrated, and stained for collagen with Masson's Trichrome stain or elastin with Verhoeff Van Gieson elastin stain kit (Polysciences Inc, Warrington, PA) according to the manufacturer's instructions. Immunohistochemical analysis was performed on the tissue on slides to determine the expression of pro-collagen I and fibronectin using the Vectastain Elite kit (Vector laboratories, Burlingame, CA). For pro-collagen I immunostaining, the tissues were subjected to antigen retrieval with citrate buffer pH 6 for 15 minutes. For both fibronectin and pro-collagen I immunostaining, the tissues were blocked with 3% of normal goat serum (Vector laboratories) in Tris-buffered saline containing 0.1% of BSA, incubated overnight at 4°C with rabbit anti-human pro-collagen I antibody (EMD, Millipore, Danvers, MA) at 1:100 or rabbit anti-human and mouse fibronectin antibody (Abcam, Cambridge, MA) at 1:200 diluted in blocking serum, incubated with the respective biotinylated secondary antibodies followed by incubation with Avidin Biotin Complex, and then, DAB substrate chromogen

system (DAKO, Santa Clara, CA). Coverslips were place on the slides and the tissues imaged using a high-resolution digital whole-slide scanning technology for brightfield system (Experimental Pathology Research Laboratory, NYU Langone Health CORE Facility (SlidePath, Leica Biosystems, Danvers, MA) was used as the digital image database.

2.4 | Cell culture and treatments

Primary human foreskin fibroblasts (HFF, CRL-2091, CCD-1070SK, American Type Culture Collection (ATCC), Manassas, VA) were cultured in Minimum Essential Medium (Gibco #10370-021, Thermo Fisher Scientific, Waltham, MA) supplemented with 10% of fetal bovine serum (Atlanta Biologicals, #S1115OH, R&D Systems, Minneapolis, MN), 1% of L-Glutamine (#25-005-CI, Corning, Inc, Corning, NY), 1 mM of sodium pyruvate solution (#11360-070, Gibco), and 1% of antibiotic-antimycotic solution (#30-001-CI, Corning). Normal adult human dermal fibroblasts (HDF; #CC-2511[from female skin], Lonza Inc, Morristown, NJ), wild-type mouse embryonic fibroblasts (K41), and calreti-culin-null mouse embryonic fibroblasts (K42; kind gift of Joanne Murphy-Ullrich, University of Alabama) were cultured in Dulbecco's Modified Eagle medium (Gibco, #11995-065, Thermo Fisher Scientific) supplemented with 10% of fetal bovine serum and 1% of antibiotic-antimycotic solution.

Cell treatments for Immunoblotting and qRT-PCR analysis were as follows: primary human foreskin fibroblasts (HFFs) and adult human dermal fibroblasts (HDFs) were seeded at 0.7×10^5 cells/ well in a 6-well plate and the mouse K41 and K42 cells were seeded at 0.5×10^5 cells/well. After 18 hours, at approximately 70% confluency, cells were washed with phosphate-buffered saline (PBS), and then, se-rum-free media. The cells were treated with increasing concentrations of CRT or TGF-β1 in cell line respective media containing 0.5% of FBS for 24 hours or at time points designated in different experiments, and whole-cell protein lysates were prepared or RNA was isolated from the cells. For protein and mRNA analyses over time (time-course), the cells were treated with CRT or TGF-β at a constant concentration in media containing 0.5% of FBS and cells harvested at the time points shown in the respective figures. In certain experiments, to determine receptor signaling identity in response to eCRT, the TGF-β receptor I kinase inhibitor, SD208 (1 μM; Tocris Biosciences) in cell line respective media containing 0.5% of FBS was added to the cells 4 hours prior to CRT or TGF-β treatments. The LRP1 antagonist RAP (50 nM, 100 nM, 250 nM, and 500 nM) was preincubated with cells for 1 hour before treatments with CRT or TGF-β1. To determine whether eCRT is internalized by CRT K42 null cells, the cells were treated with 10 ng/mL of eCRT in media containing 0.5% of FBS and cell lysates prepared at 3, 6, 12, and

24 hours post treatment. In a separate experiment, K42 cells were pretreated with 250 nM RAP for 1 hour or with an inhibitor of macropinocytosis, 20 μM Cytochalasin D (#PHZ1063; Gibco, Thermo Fisher) for 30 minutes prior to adding 10 ng/mL of eCRT for 1 hour; cell lysates were probed for human CRT"/>**b**y immunoblotting. All cell lines were shown to be mycoplasma-free by the Mycoplasma detection kit assay (MycoProbe, R&D Systems).

2.5 | Immunoblot analysis

Total cell lysates were obtained by scrapping cells on ice into iced PBS and lysing the cells in RIPA lysis buffer (50 mM Tris-HCL, pH 7.4; 1% NP-40; 0.25% Na-deoxycholate; 150 mM NaCl; and 1 mM EDTA) containing 1X protease inhibitor cocktail (#P8340, Sigma-Aldrich, St Louis, MO) and 1X phosphatase inhibitor cocktail (#5870S, Cell Signaling Technologies, St Louis, MO). Protein concentrations were determined using the Micro-BCA protein assay kit (#23235, Thermo Fischer Scientific,) and equal amounts of protein (10-15 μg) in Laemmli buffer containing 5% of β-mercaptoethanol were subjected to SDS-PAGE and transferred onto Nitrocellulose or PVDF membranes. All antibodies are listed in the Antibody Table in Supplementary Data (S1). Membranes were blocked for 1 hour with 3% of bovine serum albumin diluted in TBST (50 mM Tris-HCL, pH 7.5; 150 mM NaCl; 0.1% Tween-20) to probe for elastin, pSmad2, and pSmad3 and with 5% of milk diluted in TBST for fibronectin, collagen α1 Type I, α-smooth muscle actin, Smad2/3, integrin α5 and integrin β1, TGF-β1, TGF-β2, and TGF-β3, and then, incubated with the following antibodies overnight in 5% of nonfat dry milk in TBST at 4°C: goat anti-human collagen α1 Type I (#SC-8783, Santa Cruz Biotechnology, Dallas, TX) at 1:1000, mouse anti-human fibronectin (#610078, BD Biosciences, San Jose, CA) at 1:1000, mouse anti-human elastin (SC-166352, Santa Cruz Biotechnology) at 1:250, rabbit anti-human integrin β1(#SC-8978, Santa Cruz Biotechnology) at 1:500, rabbit anti-human integrin α5 (SC-10729, Santa Cruz Biotechnology) at 1:1000, mouse anti- human α-smooth muscle actin (#A5228, Sigma Aldrich) at 1:500, rabbit anti-human-pSmad2 (Calbiochem, #566415, EMD Millipore) at 1:1000, rabbit anti-human pSmad3 (#ab52903, Abcam) at 1:1000, and rabbit anti-human Smad2/3 (#3102S, Cell Signaling Technologies) at 1:1000. For experiments analyzing eCRT internalization in K42 CRT null MEFs, cell lysates (10 μg) were subjected to SDS-PAGE (10% acrylamide) and transferred to a PVDF membrane (Amersham HyBond, GE Healthcare). The membrane was blocked in 5% of nonfat milk for 1 hour, incubated with anti-CRT monoclonal antibody at 1:1000 (ADI-SPA-601-D, Enzo Life Sciences, Farmingdale NY) in 5% of nonfat milk overnight at 4°C, followed by incubation with peroxidase-conjugated goat anti-mouse (1;2000; #23430, Invitrogen, Thermo Fisher Scientific) in TBST for 90 minutes.

To detect TGF-β isoforms for experiments shown in Figure 5, Figure 8, and Figure 7D for TGF-β3, 15-20 μg total protein per well was subjected to SDS-PAGE containing 12% of acrylamide or a 5%-20% of acrylamide gradient and transferred to a PVDF membrane. The antibodies used were rabbit anti-human non-cross-reacting anti-peptide antibodies (purified IgG) to the three mammalian TGF-β isoforms (TGF-β1, TGF-β2, TGF-β3), as described.[52] The membrane was blocked in 5% of non-fat milk overnight at 4°C. Each antibody at a concentration of 2-8 μg/mL in 3% of nonfat milk in TBST was incubated with the membrane overnight at 4°C or for 4 hours at room temperature. For the blots using mouse embryo fibroblasts, K41 (WT) and K42 (CRT$^{-/-}$) that were treated with eCRT, the following antibodies in 5% of nonfat dry milk in TBST were incubated with the membrane over night at 4°C: rabbit anti-mouse collagen I (#AB765P, Millipore) at 1:500 in TBST, rabbit anti-mouse elastin (#MBS821275, MyBioSource, Ann Arbor, MI) at 1:200 in TBST, mouse anti-mouse fibronectin (#610078, BD Biosciences) at 1:500 in TBST and anti-mouse integrin α5 (SC-10729, Santa Cruz Biotechnology) at 1:500 in TBST.

To control for equal loading in each well, mouse anti-human and mouse β-actin (#A1978, Sigma Aldrich) at a concentration of 1:40 000 in TBST was used for membranes containing 20 μg of protein and at 1:10 000 for all others. Following washing three times TBST, all membranes were treated with peroxidase-conjugated secondary antibodies to the species immunized for each respective antibody for 1.5 hours, according to the following conditions: goat anti-rabbit (#324360, Invitrogen Thermo Fisher Scientific) at 1:2000 in TBST, goat anti-mouse (#32430, Invitrogen, Thermo Fisher Scientific) at 1:2000 in TBST and donkey anti-goat (#SC2020, Santa Cruz Biotechnology) at 1:5000 in 5% of milk diluted in TBST. Proteins on the membranes were detected by chemiluminescence using either ECL western blotting substrate (#32209, Thermo Fisher Scientific) or SuperSignal West Dura Extended Duration Substrate (#34075, Thermo Fisher Scientific) followed by autoradiography (#E3218, Denville Scientific, Metuchen, NJ) and the films scanned using an Office-jet scanner. The density of each band was determined using Image-J software (NIH). The values shown below each well in all immunoblots represent the intensity of each band compared to 1.0 representing the untreated control and normalized to the corresponding intensity of β-actin in the same well.

2.6 | Quantitative real-time PCR

Cells were plated as described above and neonatal human foreskin fibroblasts (HFF) and adult human dermal fibroblasts (HDF) were plated at concentration 0.7×10^5 cells/well in a 6-well dish treated with CRT and TGF-β1 in cell respective media containing 0.5% of FBS until approximately 70% confluent, usually 24 hours after seeding. Total

RNA was isolated using RNeasy Mini kit (#74104, Qiagen, Germantown, MD) as per manufacturer's protocol, the RNA quantified by NanoDrop (Thermo Fisher Scientific) and cDNA synthesized using iScript reverse transcription kit (#1708841, Bio-Rad, Hercules, CA). Quantitative RT-PCR was performed using iTaq universal SYBR Green Supermix (172-5121, Bio-Rad) and a CFX96 Touch Real-Time PCR Detection System (Bio-Rad). Primer sequences are listed in the Primer Table in Supplementary Data (S2). Amplifications were carried out with an initial denaturation at 95°C for 3 minutes, followed by 40 cycles of 95°C for 10 seconds and 60°C for 30 seconds. Values were normalized to GAPDH as an internal loading control and fold change compared to untreated controls were calculated using the $\Delta\Delta C_t$ method.

2.7 | Magnetic Luminex Performance assay to determine TGF-β1 in cell supernatants

The levels of TGF-β1 protein released into supernatants following treatment of HFFs CRT were determined by Magnetic Luminex Performance assay kit (#FCSTM17, R&D Biosystems). Cells were seeded at 3,300 cells/well in a 96-well plate, incubated for 24 hours, washed once with PBS, and treated with increasing concentrations of CRT (0-100 ng/mL) in MEM media containing 0.5% of FBS. To determine whether CRT induced TGF-β1 release by LRP1 signaling, cells were preincubated with RAP (50 nM, 100 nM, and 250 nM, 500 nM) for 60 minutes prior to treatment with of CRT. The samples were prepared according to manufacturer's instructions. Briefly, after 24 hours treatment, cell supernatants were centrifuged at 400 X g for 5 minutes, Latent TGF-β1 in the supernatants was activated by adding 20 μL of 1 N HCl to 100 μL sample, incubating for 10 minutes at room temperature, adding 20 μL of 1.2 N NaOH/0.5 M HEPES with mixing, and finally, 100 μL of the mixture were subjected to the Magnetic Luminex assay. The assay was quantified using Luminex MAGPIX analyzer (Thermo Fisher Scientific). Concentration of TGF-β1 protein in each supernatant sample was calculated from a standard curve of increasing concentrations of activated TGFβ1 provided with the kit.

2.8 | Determination of amount of ECM and TGF-β proteins released into supernatants over time

HFFs were seeded at 0.7×10^5 cells/well in a 6-well plate and after 24 hours, the cells were washed once with PBS, once with serum free media, subsequently treated with CRT (10 ng/mL) in 10 mL of MEM media containing 0.5% of FBS, and cell supernatants collected at points over time (3-48 hours). The cell supernatants were collected, pipetted into dialysis membranes (Spectra/por3, 3.5 kDa molecular weight cutoff,
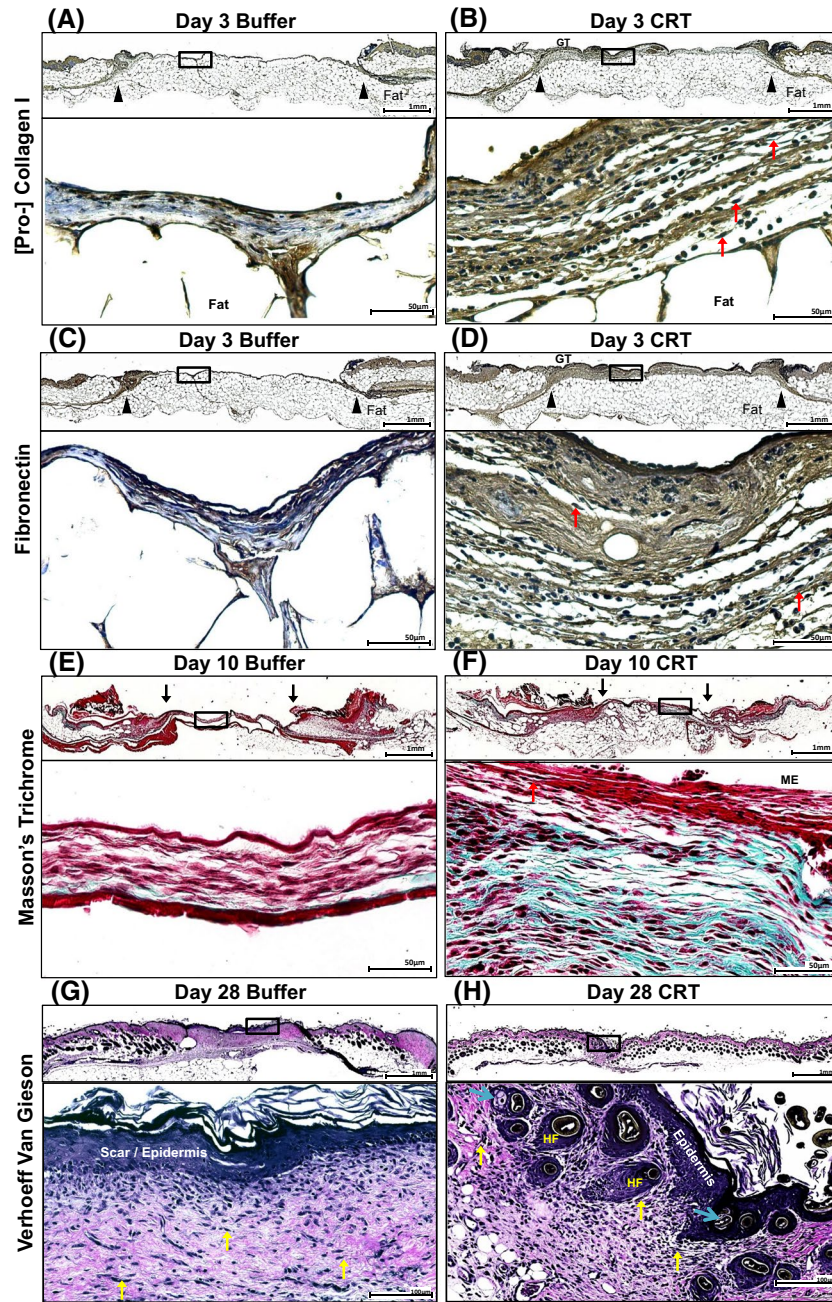
FIGURE 1 Topical application of calreticulin (CRT) to cutaneous wounds of diabetic (db/db) mice induces granulation tissue formation and increased expression of ECM proteins. Tissues from full-thickness wounds from the dorsal skin of leptin receptor-deficient (db/db) mice were treated with 10 μL of 5.0 mg/mL CRT for four consecutive days (total 200 μg), the wounds excised into 10% of neutral formalin, cut to 5.0 μm on slides and subjected to immunohistochemical analysis (IHC) for collagen type I or fibronectin, or stained for elastin with Verhoeff Van Gieson stain. CRT-treated wounds exhibited earlier tissue maturation and more abundant granulation tissue (GT) observed from day 3 through day 28 post-wounding than the tris-buffered saline-treated control (Buffer). (A) Day 3 post-wounding buffer-treated wound and (B) CRT-treated wound. Red arrows: fibroblast-like cells; Brown: positive staining for procollagen I; Blue: cell nuclei. (C) Day 3 post-wounding buffer-treated wound and (D) CRT-treated wound; Brown stain: intracellular and extracellular fibronectin. Top panels 1.66× magnification, scale bar: 1 mm; Bottom panel: 40× magnification, scale bar: 50 μm. (E)10 days post-injury buffer-treated wound and (F) CRT-treated wound stained with Masson's Trichrome stain. Cyano: collagen; Dark red-black: cell nuclei; Red: muscle fibers, cytoplasm, keratin. Top panel: 1.66× magnification, scale bar: 1 mm; Bottom panel: 40× magnification, scale bar: 50 μm. Complete wound closure of the wounds occurred approximately by day 14 post-wounding. (G) 28 days post-wounding buffer-treated wound and CRT-treated wound (H) stained for elastin fibers with Verhoeff Van Gieson stain. (G) Buffer-treated wound illustrates hypertrophic epidermis and scar tissue with no epidermal appendages in the wound area. (H) CRT-treated wounds resemble unwounded skin with regeneration of dark-pigmented hair follicles (HF), sebaceous glands (blue arrows), and abundant elastin-rich fibers. Dark blue-black fibers = elastin fibers (yellow arrows). Top panel: 1.66× magnification, scale bar: 1 mm; Bottom panel: 20× magnification, scale bar: 100 μm. GT = granulation tissue; HF = hair follicle. Black arrows on 1.66× magnification images (A to F top panel) indicate the wound margin

HFF, 24h
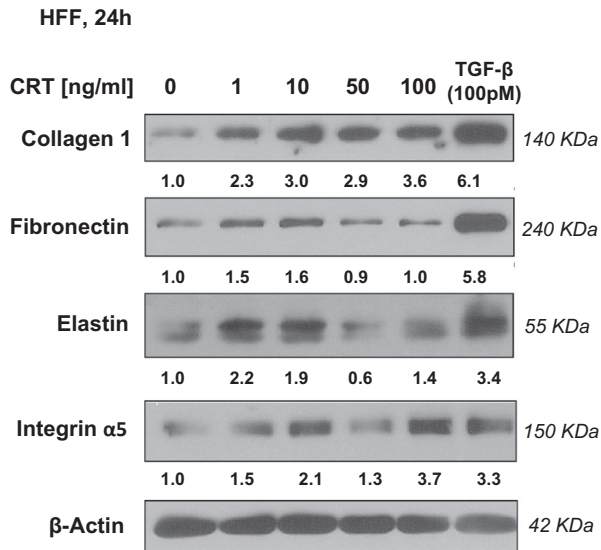
FIGURE 2 Exogenous CRT induces ECM proteins and α-5 integrin by human fibroblasts. Human foreskin fibroblasts (HFF) were treated with increasing doses of eCRT (0-100 ng/mL [2000 pM]) or TGF-β1 (100 pM) in MEM containing 0.5% of FBS. After 24 hours, cell protein lysates were collected in iced RIPA lysis buffer, protein concentrations determined by MicroBCA assay kit, equal amounts of protein (15 μg) in Laemmli sample buffer (reduced) applied to 10% of acrylamide SDS-PAGE, proteins transferred to a nitrocellulose membrane, and the membranes probed with antibodies to collagen I, fibronectin, elastin, and integrin α5 (details in Supplementary Antibody Table; S1). eCRT induces collagen I, fibronectin, elastin, and α5 integrin. The membranes were exposed to autoradiography film, densitometrically scanned, and levels of protein in each well quantified using Image-J. The values shown below each well represent the intensity of each band compared to 1.0 representing the untreated control and normalized to the corresponding intensity of β-actin. Representative blot of n = 8

of FBS served as negative control. Cell proliferation was determined using the WST-8 Cell Proliferation Assay (Dojindo Molecular Tech Inc, Rockville, MD). Live cell numbers were determined by adding 10 μL [2-(2-methoxy-4-nitrophenyl)-3-(4-nitrophenyl)-5-(2,4-disulfophenyl)-2H-tetrazolium to each well. After 1 hour, absorbance was measured at 450 nm using a microplate reader (Bio-Rad 680).

2.10 | Cellular migration determined by the in vitro wound healing scratch plate assay

Wild-type (WT) and calreticulin-deficient (CRT$^{-/-}$) mouse embryonic fibroblasts (MEF) were seeded onto 24-well plates at a density of 1×10^4 cells/well in Dulbecco's Modified Eagle medium containing 10% of FBS. The wound healing scratch plate assay was performed as previously described.[22] Briefly, at approximately 70% confluency, cells in the middle of the plate were removed by drawing a line with a 200 μL pipette tip. The plate was washed with PBS and the cells treated for 24 hours with increasing concentrations of CRT (0-100 ng/mL) in media containing 0.5% of FBS or medium alone containing 0.5% of FBS as a negative control. Cells were stained at time 0 and 24 hours with 0.025% of Coomassie blue stain in 10% of acetic acid, 45% of methanol for 15 minutes, and images of each plate captured using an inverted microscope (Olympus CK, Tokyo, Japan) Cell migration was calculated by measuring the area of the gap (pixels^2) in each well and comparing each value with the corresponding original scratch area at time zero. Measurements were normalized for cell density using an area of the plate that was distal and lateral to the scratch.

2.11 | Statistical analysis

Results are presented as mean $\pm$ SD or $\pm$ SE. Statistical analysis was performed by either two-tailed, unpaired Student's t tests for comparisons between two means, or one-way analysis of variance (ANOVA) for comparisons between more than two means, using GraphPad Prism software. Statistical significance was defined as $P \le .05$ at 95% confidence level. Statistics are specified in individual figure legends.

(#132720T, Spectrum Chemicals Manufacturing Corporation, New Brunswick, NJ), and dialyzed overnight in 2 L of 0.001 M Tris-HCl, pH 7.4 at 4°C with three buffer changes, lyophilized, and resuspended in 100 μL in distilled deionized sterile water. Protein concentrations were quantified by Micro BCA protein assay kit (Thermo Fisher Scientific) and 40 μg of protein/well subjected to SDS-PAGE (12% acrylamide) followed by immunoblotting with antibodies, as described above.

3 | RESULTS

3.1 | Topical treatment of calreticulin on diabetic mouse excisional wounds increases collagen, fibronectin, and elastin for abundant granulation tissue

In previous studies, using a diabetic mouse model (db/db) of cutaneous excisional wound repair, we showed that topical application of calreticulin (CRT) for four consecutive

2.9 | In vitro assay for cellular proliferation

Wild-type (WT) and calreticulin-null (CRT$^{-/-}$) mouse embryonic fibroblasts (MEF) were seeded onto 96-well plates at a density of 500 cells/well in Dulbecco's Modified Eagle medium containing 10% of FBS. Cells were grown to approximately 50% confluency, washed, and switched to medium containing 0.5% of FBS for 24 hours. Increasing concentrations of human CRT were added to the cells in 0.5% of FBS medium and the cells incubated for 48 hours; medium containing 0.5%

days post-wounding increased the rate and quality of wound healing including regeneration of epidermal appendages and lack of scarring compared to buffer-treated controls.[22] Thus, CRT induces wound healing by a tissue regenerative process. Importantly, CRT corrected most of defects associated with the poor healing of human chronic diabetic wounds including lack of cell recruitment, impaired cell proliferation, and paucity of granulation tissue (GT) formation.[22,24] As shown in Figure 1B,D, granulation tissue was observed in the wound bed on top of fat by 3 days post-wounding (CRT, right), whereas buffer-treated wounds (left) showed scant granulation tissue (Figure 1A,C). At this time point, increased

(A) HFF, 24h

(B) HDF, 24h

(C) HFF, 24h — mRNA levels

(D) HDF, 24h — mRNA levels

* t test p<0.05 CRT and TGFb vs Untreated
# t test p<0.05 All treatments vs corresponding SD208
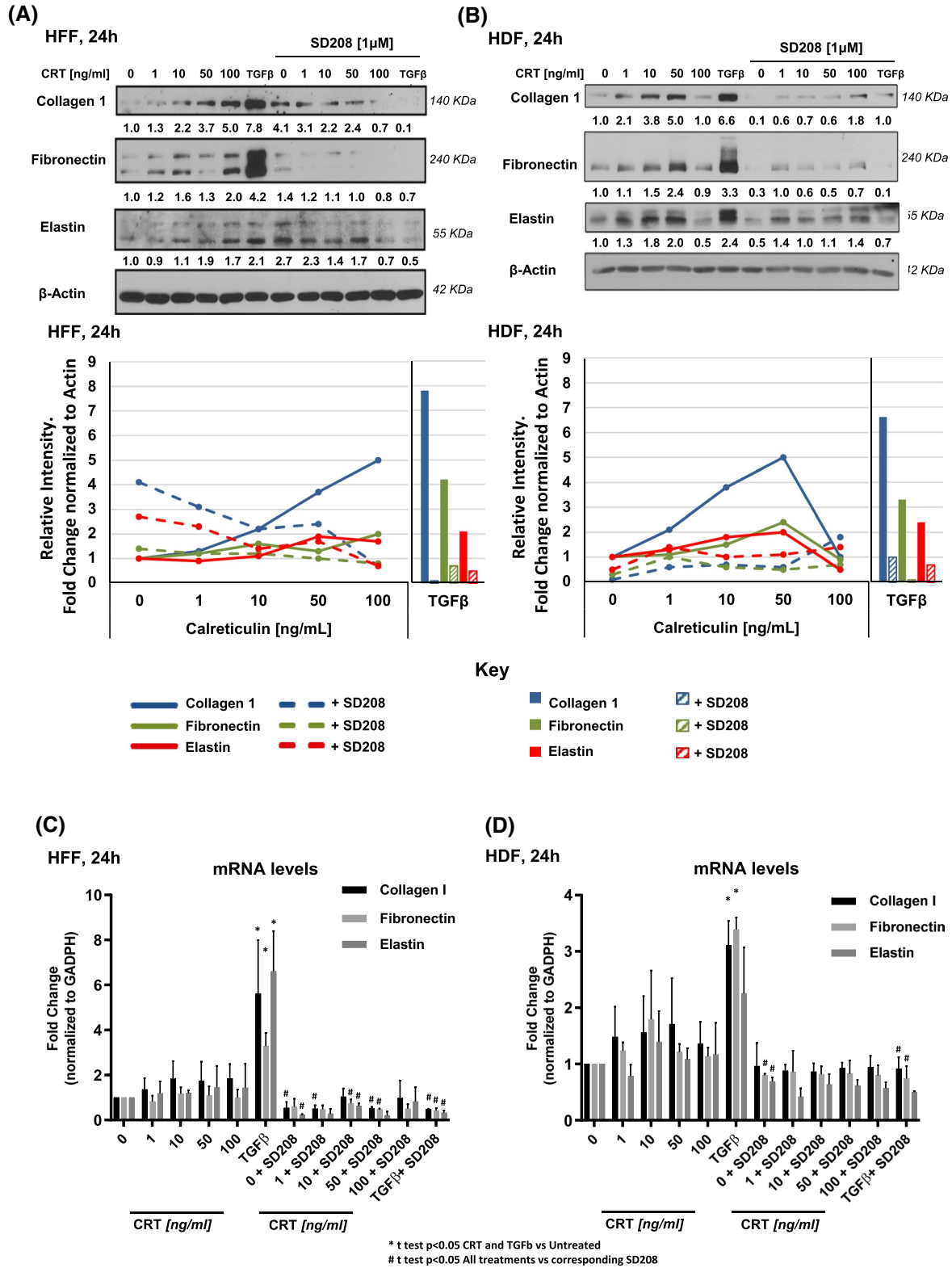
FIGURE 3 Exogenous CRT induction of ECM and α-SMA proteins and mRNA is mediated by TGF-β signaling in human neonatal and adult dermal fibroblasts. Human foreskin fibroblasts (HFF) and normal human dermal fibroblasts (HDF) in their respective media containing 0.5% of FBS were treated with increasing doses of eCRT (0-100 ng/mL) or TGF-β1 (100 pM), in the presence or absence of the TGF-β receptor I serine/threonine kinase inhibitor SD208, added 4 hours prior to eCRT or TGF-β. After 24 hours, cell protein lysates were prepared in iced RIPA buffer or total RNA was isolated with RNeasy, and immunoblotting (details in Supplementary Antibody Table; S2) or q-RT-PCR (details in Supplementary Primer Table; S2) was performed, respectively. Cell lysates (10-20 μg) were applied to SDS-PAGE (Panel A: HFF; 7.5% acrylamide) Panel B: HDF; 10% acrylamide) followed by transfer to a nitrocellulose membrane for immunoblotting. Panel C: HFF mRNA and Panel D: HDF mRNA. Statistical significance between untreated and TGFβ-treated was estimated by unpaired Student's *t* test *$P \le .05$; Statistical significance between cells treated with eCRT or TGF-β1 and SD208 inhibition of mRNA transcription was estimated by unpaired Student's *t* test #$P \le .05$. Panel E: α-SMA in HFFs (10% acrylamide); Panel F: α-SMA mRNA in HFFs. Panel G: Collagen and fibronectin induction and Smad2P activation (p-Smad2). Panel H: p-Smad3 activation and in the same experiment increased fibronectin and collagen, which all were inhibited by SD208. Induction of ECM proteins and α-SMA is mediated by TGF-β canonical signaling with varying dependencies. Autoradiography films were quantified using Image-J; densitometries were normalized to the corresponding intensity of β-actin and compared to untreated control set at one. Densitometry values are shown below each well and represented in the linear graph below each immunoblot. The levels of ECM induction by TGF-β are shown in the adjacent bar graph collagen I, blue; fibronectin, green; elastin, red. q-RT-PCR values were normalized to GAPDH, fold-change was calculated using ΔΔCt method and normalized to the untreated control. Mean values ± Standard Deviation (SD) are represented in bar graphs (Panels C and D). All immunoblots and qRT-PCR graphs are representative of n = 3-4

immunohistochemical staining for procollagen I (Figure 1B; brown stain) and fibronectin (Figure 1D; brown stain) was observed including numerous fibroblasts (red arrows) in the granulation tissue of the wounds treated with CRT. By day 10 post-wounding (Figure 1F), numerous collagen fibrils (cyano) and a highly cellular (red nuclei) neodermis, largely composed of fibroblasts, identified by their elongated polygonal shape (red arrows), are shown by Masson Trichrome staining in the CRT-treated wounds. In contrast, the buffer-treated wounds, comparatively, showed a negligible amount of collagen fibrils and less cells (Figure 1E). Example of the neogenic induction of epidermal appendages, hair follicles (HF; yellow), and sebaceous glands (SG; blue arrows) are observed in the CRT-treated wounds shown here after 28 days of healing (Figure 1H). This is in sharp contrast to the scar and hypertrophic epidermis shown for the buffer-treated wound at both low (1.66×) and high magnification (40×) (Figure 1G). However, as shown under low power (Figure 1G; upper left panel) hair follicles are observed in the adjacent unwounded skin on either side of the scar/hypertrophic epidermis. Of note, the neogenic hair follicles contained pigmented [black] hair (HF), which has not been observed before in adult mammals following full-thickness cutaneous injury (Figure 1H). By Verhoeff Van Gieson staining, contrasting to the buffer-treated wounds (Figure 1G; left panel), a higher density of abundant dark blue-black dense elastin fibers (yellow arrows) in the CRT-treated wounds was observed (Figure 1H); right panel); collagen is stained pink. In summary, a greater amount of granulation tissue replete with epidermal appendages was observed in the calreticulin treated excisional mouse wounds (right panels) compared to buffer-treated controls (left panels). Although there might be subtle differences, the results observed are likely not female-dependent as another study showed that treatment of male rats with *Trypanosoma Cruzi* CRT enhanced cutaneous wound healing.[53]

3.2 | Exogenous calreticulin induces ECM proteins and α-5 integrin by human fibroblasts

To identify ECM and other proteins important in wound repair that are induced by extracellular CRT (eCRT), human neonatal foreskin fibroblasts (HFF) were treated with increasing doses of eCRT (0-100 ng/mL) for 24 hours and protein levels determined by immunoblotting. TGF-β (100 pM), a notably strong inducer of ECM proteins was used as a positive control.[37,54-57] Figure 2 shows that eCRT dose-dependently induces collagen I, fibronectin, elastin, and α5 integrin in HFFs. As determined by densitometric scanning of the protein bands in each lane, fold induction is shown below each lane for this representative blot. eCRT protein induction ranged between 3.6 and 2.2 with collagen I the most highly induced and elastin the least. The decrease in fibronectin at 50 ng/mL was consistently observed in HFFs. Notably, 100 pM TGF-β induced stronger expression of ECM proteins at molar concentration of 2-20 times more than eCRT. For example, a 20-fold higher concentration of TGF-β (100 pM) compared to eCRT (100 ng/mL; 2,000 pM) induced nearly twice as much collagen.

3.3 | The induction of the extracellular matrix proteins, collagen I, fibronectin, and elastin by calreticulin is mediated by TGF-β signaling in human dermal fibroblasts

Since TGF-β potently induces ECM protein synthesis, which is broadly responsible for fibrosis of many human organs including lung and kidney and cutaneous scarring,[9,37,38,40,41,46,58,59] we proposed that eCRT might exploit TGF-β for ECM induction. To test this hypothesis, both eCRT-treated HFFs and human adult dermal fibroblasts (HDFs) were analyzed for ECM mRNA and protein expression in the presence or absence of the specific

(E)

HFF, 24h

(F)

HFF, 24h

mRNA levels

HFF, 24h

(G)

HFF, 24h

(H)

HFF, 24h
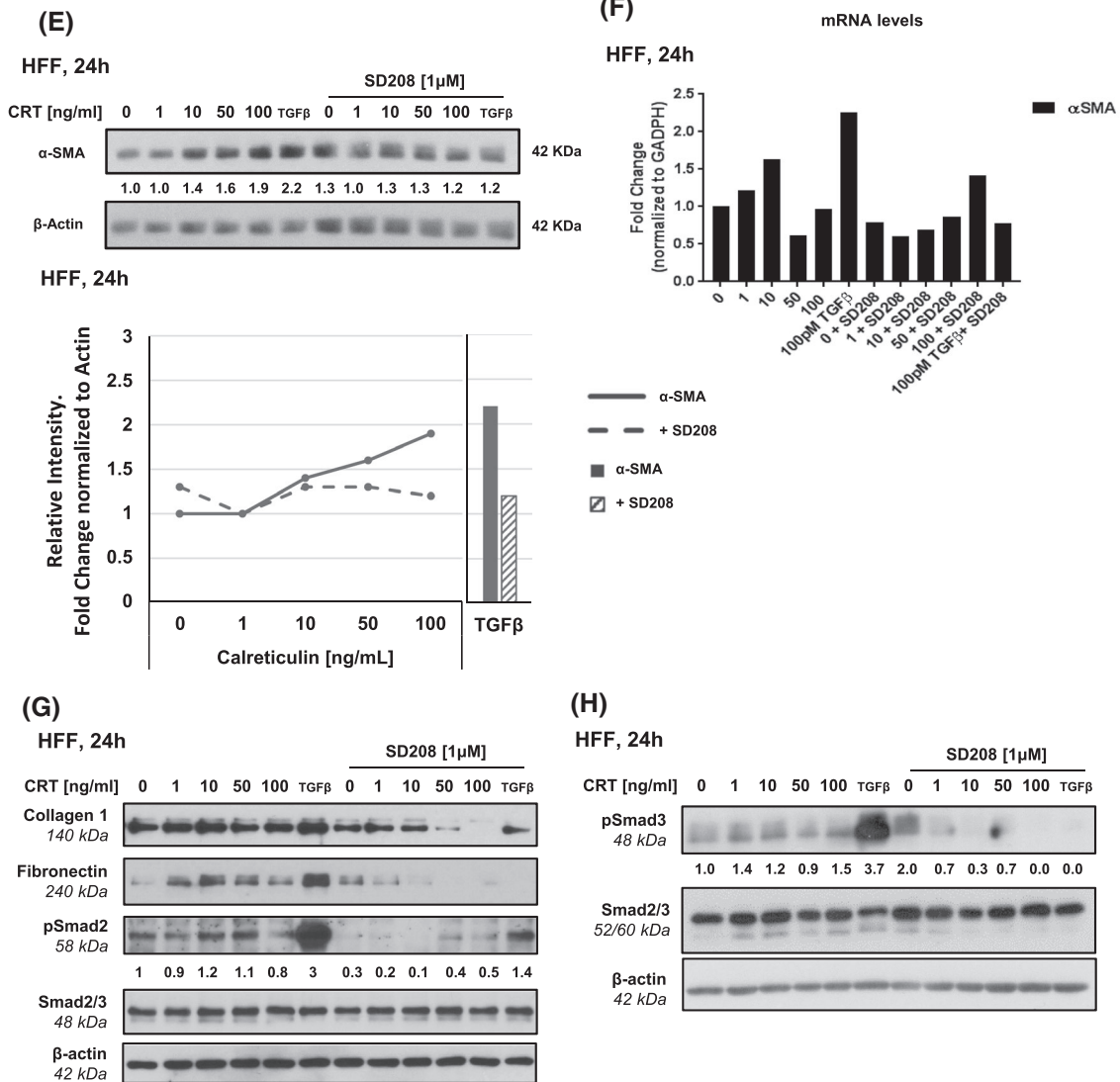
FIGURE 3 Continued

serine-threonine kinase inhibitor of TβRI signaling, SD208. As shown in the representative immunoblot in Figure 3A (left), similar to Figure 2, following treatment of neonatal HFFs with increasing doses of eCRT (0-100 ng/mL) for 24 hours, a dose-dependent increase in collagen, fibronectin, and elastin was obtained between 2.0 and 5.0-fold at 100 ng/mL eCRT. Similarly, as shown in Figure 3B (right), a dose-dependent response in the induction of collagen, fibronectin, and elastin, was obtained following treatment of adult HDFs with eCRT showing peak responses between 2.0 and 5.0-fold at 50 ng/mL eCRT. Collagen I protein induction by TGF-β was 7.8 and 6.6-fold higher than eCRT in HFFs and HDFs, respectively. Notably, the pretreatment of both HFFs and HDFs for 4 hours with the TβRI kinase inhibitor, SD208, either partially or completely blocked eCRT induction of ECM proteins in both cell lines, confirming that eCRT induction of ECM proteins is mediated largely or completely by TGF-β canonical signaling (Figure 3A,B, right part

of blots). However, the increase in elastin levels in both cell lines, and collagen I in HFFs, induced by eCRT was not fully blocked. Therefore, there appears to be activation of (a) signaling pathway(s) in addition to TGF-β canonical signaling for collagen I in HFFs and elastin induction by eCRT for both cell lines. Interestingly, the addition of SD208 to untreated HFFs resulted in an increase in collagen I and elastin over the untreated control. Both the subtle and more obvious differences observed between HFFs [male] and HDFs [female] might be related to both sex difference and neonatal vs adult fibroblast responses. As shown in Figure 3C (HFFs) and Figure 3D (HDFs), from the same eCRT-treated cell cultures, a less robust response in the levels of mRNA for collagen 1, fibronectin, and elastin (1.5 to 2-fold) than for the proteins was obtained (not statistically significant compared to untreated controls; $P \leq .07$). Compared to eCRT, the induction of transcription of the ECM proteins by TGF-β was 2.1-7.8 and 2.4-6.6 (elastin is the lowest number)

(A)

HFF, 24h

(B)

HDF, 24h
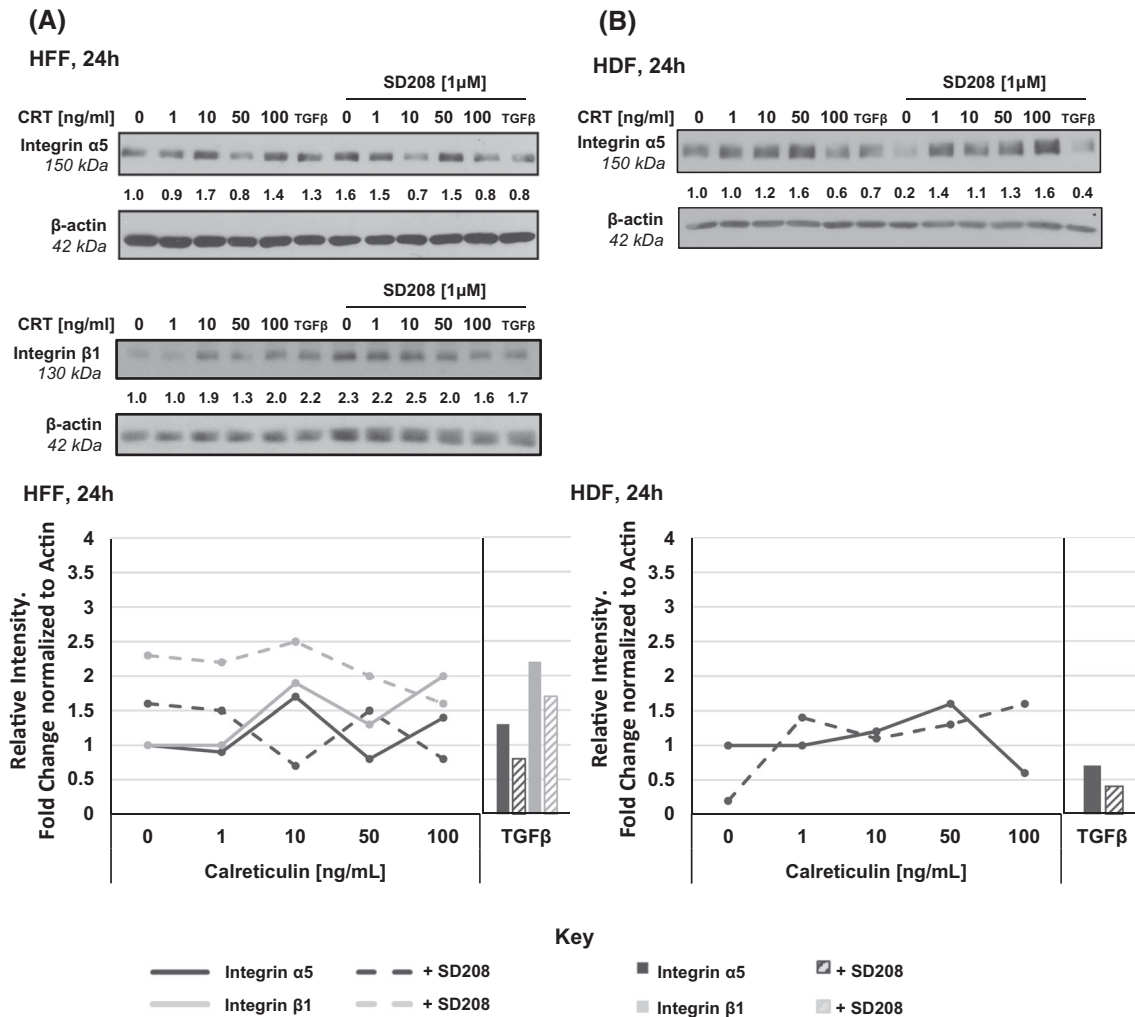
FIGURE 4 Exogenous CRT induction of α-5 and β-1 integrin is independent of TGF-β signaling in human neonatal and adult dermal fibroblasts. Human foreskin fibroblasts (HFF) and normal human dermal fibroblasts (HDF) were treated with increasing doses of eCRT or TGF-β1 (100 pM), in the presence or absence of the TGF-β receptor I serine threonine kinase blocker, SD208. After 24 hours, whole-cell protein lysates were prepared with iced RIPA buffer and immunoblotting (Antibody Table) was performed. Panel A: HFF, immunoblot of α5 (top) and β1 (bottom); Panel B: HDF, immunoblot of α5. The immunoblots are representative of n = 3. Scanned autoradiography films were quantified using Image-J and densitometries were normalized to the corresponding intensity of β-actin and compared to untreated control with a value of 1.0. Densitometries are shown below each well and are represented by the linear graph below the blots and adjacent bar graphs showing TGF-β1 effects (integrin α5, dark gray; integrin β1, light gray)

higher in HFFs and HDFs, respectively (≤.01). As shown for protein induction, the low level of transcription of ECM mRNA by both eCRT and TGF-β was inhibited by SD208.

TGF-β has been shown to induce α-smooth muscle actin (α-SMA) as a marker for myofibroblast differentiation, important in wound contraction. As shown in Figure 3E, adose-dependent increase of α-SMA protein was observed following treatment of HFFs with eCRT (0-100 ng/mL) with a peak response of 1.9-fold at 100 ng/mL, which was inhibited by SD208 by comparison with the SD208 alone control. As observed for collagen I and elastin protein levels (Figure 3A,B), SD208 alone increased α-SMA (30%). As shown for the ECM proteins (Figure 3C,D), the levels of α-SMA mRNA induced by eCRT were less robust than the protein response (Figure 3E). TGF-β induced mRNA

levels were more than twice as high compared to CRT (albeit still low).

In response to eCRT, both the downstream Smad2 and Smad3 transcription factors for TGF-β canonical signaling were phosphorylated by TβRI kinase. However, Smad2 was only slightly phosphorylated and Smad3 moderately phosphorylated by eCRT treatment in HFFs compared to the levels of unphosphorylated Smad2/3 (Figure 3F,G), which remain unchanged. As shown in Figure 3A, the induction of fibronectin by eCRT was completely inhibited by SD208, whereas collagen was partially inhibited or the increase observed is related to super-induction of this protein by the inhibitor. Similar to the ECM protein responses to 100 pM TGF-β and compared to eCRT, pSmad2 (3.0 vs 1.2-fold) and pSmad3 (3.7-fold vs 1.5) phosphorylation levels

(A)

HFF, 24h

(B)

ELISA. TGF-β1 release into media

HFF, 24h

(C)

HFF, Time course
Supernatants


(D)

HFF, Time course
Lysates
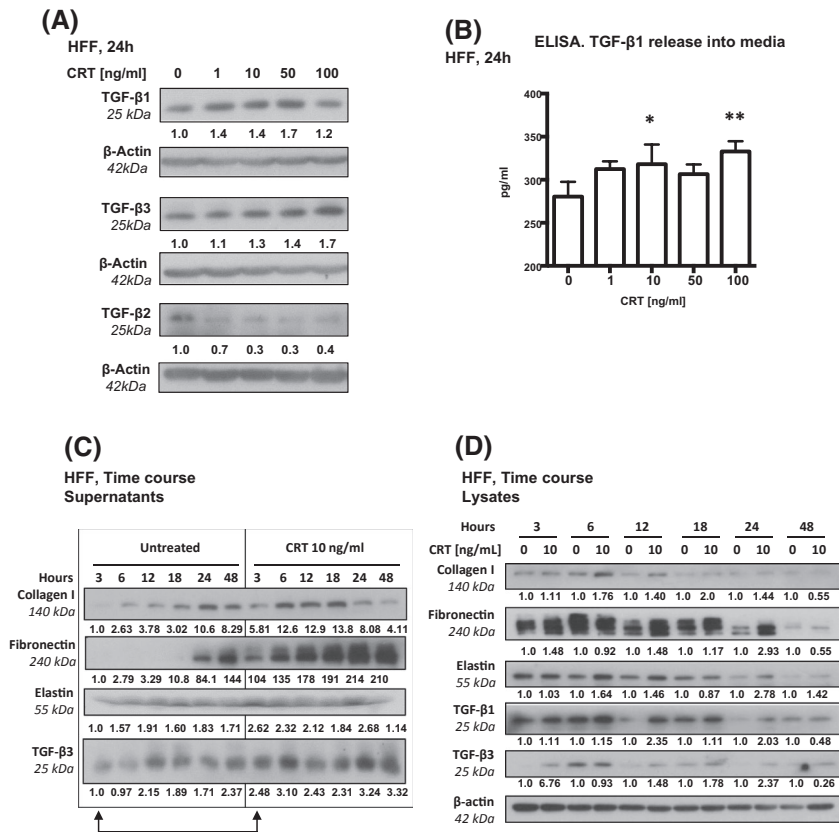
FIGURE 5 CRT induces TGF-β3 protein expression and release prior to induction of ECM and TGF-β1 proteins by human dermal fibroblasts. HFFs were treated with increasing doses of eCRT in the presence of 0.5% of serum for 24 hours, protein lysates prepared with iced RIPA buffer, and equal amounts of protein were loaded into each well of a 10%-20% of gradient SDS-PAGE, transferred to a PVDF membrane, and subjected to immunoblotting with isoform-specific anti-TGF-β 1, 2, and 3 purified IgG (details in: Supplemental Antibody Table; S1). Panel A: HFFs, immunoblot for TGF-β isoforms 1, 2, and 3 (n = 4). Panel B: HFFs were seeded at 3×10^3 cells/well in a 96-well plate, treated with eCRT in media containing 0.5% of FBS. After 24 hours, supernatants were collected and 100 μL supernatants in triplicate were assayed by a TGF-β1 ELISA kit (Magnetic Luminex Assay). Data were analyzed by one-way ANOVA: untreated vs 10 ng/mL CRT (*$P < .05$) and 100 ng/mL CRT (**$P < .01$; Mean ± SD (n = 2-3). Panels C and D: HFFs were treated with eCRT (10 ng/mL) or untreated, as described in Panel A, and supernatants and cell lysates from the same samples collected after 3, 6, 12, 18, 24, and 48 hours. Panel C: Supernatants from each treatment parameter were dialyzed, lyophilized, diluted, and 40 μg of protein subjected to immunoblotting for ECM proteins and TGF-β3 (n = 1). Panel D: Cell lysates (40 μg) were loaded onto a 5%-20% of acrylamide gradient SDS-PAGE and transferred to a nitrocellulose membrane for immunoblotting using anti-TGF-β1 and anti-TGF-β3 isoform antibodies, described in Pelton et al[52]. Although reduced by β-mercaptoethanol, TGF-β1 and TGF-β3 consistently electrophorese at the 25 KDa dimer when isolated from fibroblasts. Protein levels were determined by densitometry using Image-J software of scanned autoradiography films normalized to β-actin for each well and compared with untreated 3 hours for Panel C and with the corresponding untreated for each time point for Panel D assigned a value of one. Densitometry values are shown below each well. All immunoblots are representative of n = 3

were higher than the most potent dose of eCRT (10-100 ng/mL [20-2000 pM]). Phosphorylation of both Smads was not dose-dependent. Inhibition of TβRI/Smad signaling by SD208 super-induced Smad3 (compare zero untreated to treated for HFFs). Nonetheless, these data suggest TGF-β canonical signaling is involved in the mechanism for CRT induction of collagen I, fibronectin, elastin, and α-SMA. However, SD208 abrogates TGF-β-induced phosphorylation of Smad3 (Figure 3G), whereas TGF-β activation of pSmad2 (Figure 3F) and eCRT-induced responses, except for fibronectin (Figure 3A), are not fully inhibited suggesting complex signaling networks for both CRT and TGF-β in these cells (Figure 3A,B,E).

3.4 | The induction of integrins by calreticulin involves signaling mechanisms independent of TGF-β signaling in human dermal fibroblasts

As shown in Figure 2A, eCRT induces expression of α5 integrin in a biphasic manner in HFF cells. Since eCRT induces fibronectin, the matrix substrate that binds to the α5β1 integrin pair, the induction of both the fibronectin matrix and the specific integrin might be a mechanism for CRT-mediated keratinocyte migration and fibroblast recruitment into the wound.[22,23] As an interaction between TGF-β signaling and integrins has been shown,[60,61]

(A)
HFF, 24h

CRT [ng/ml]	0		10			TGF-β	
RAP	-	++	-	+	++	-	++

Collagen I
140 kDa

1.0	2.2	2.9	2.5	1.3	2.6	2.6

Fibronectin
240 kDa

1.0	0.8	1.9	0.2	1.1	2.7	2.5

Elastin
55 kDa

1.0	1.9	3.1	2.5	3.2	4.6	7.7

Integrin α5
150 kDa

1.0	1.0	1.6	1.8	2.3	1.5	2.1

β-Actin
42 kDa

(B)
HFF, 24h

CRT [ng/mL]	0	10	TGFβ	0	10	TGFβ
RAP	-	-	-	++	++	++

Collagen I
140 kDa

1.0	1.4	2.7	0.4	0.4	3.2

pSmad2
58 kDa

1.0	1.7	10.3	3.4	2.2	14.6

β-Actin
42 kDa

(C)
HFF, 24h
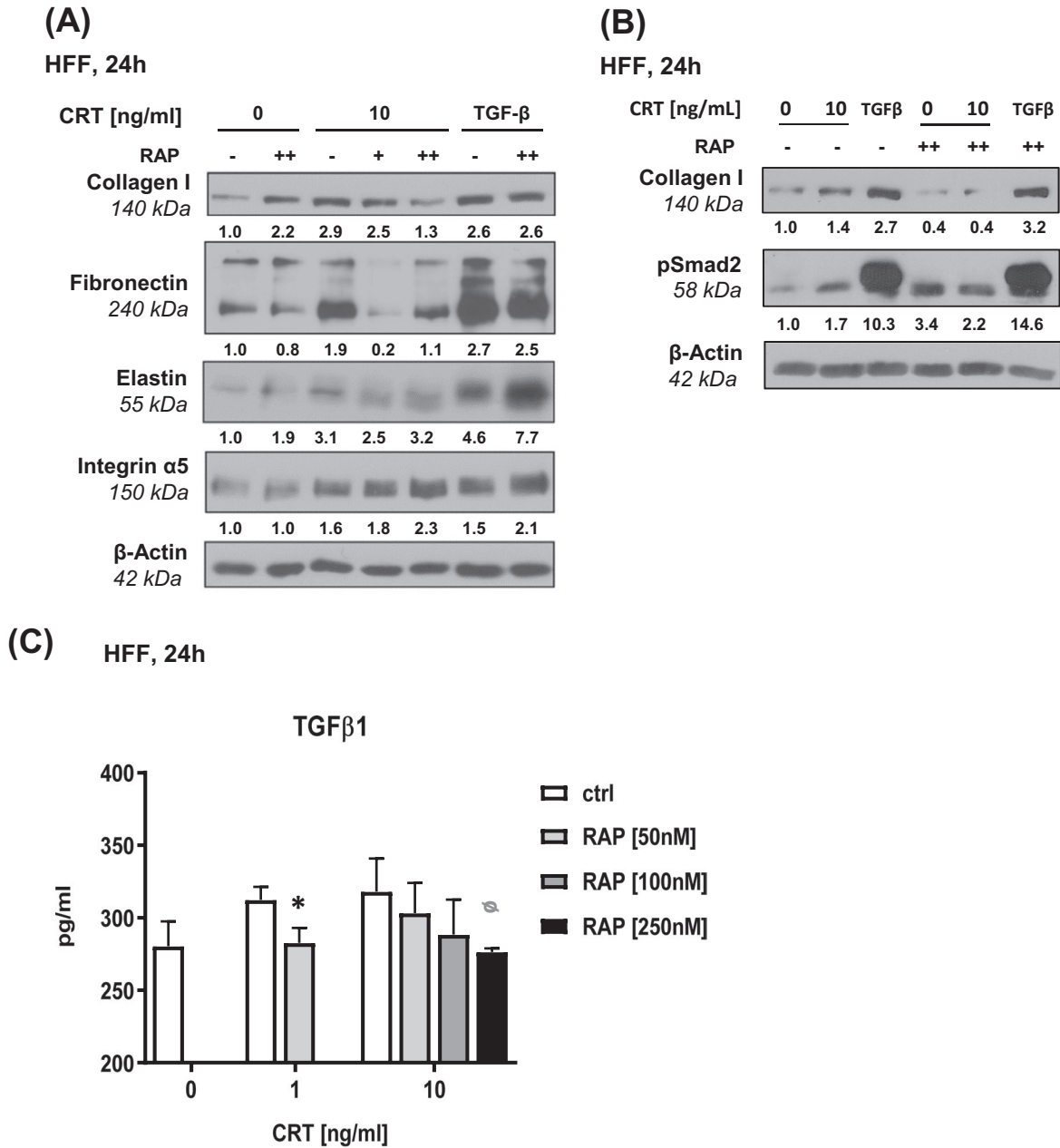
FIGURE 6 Exogenous CRT induces ECM protein expression and TGF-β1 release but not integrin α5 protein via LRP receptor signaling in human neonatal fibroblasts. Receptor-Associated Protein (RAP) binds to LRP1 and other LDL receptor family members, antagonizing ligand binding.[63-66] Panel A: HFFs were treated with or without 250 nM (+) or 500 nM (++) RAP 1 hour prior to treatment with 10 ng/mL [200 pM] eCRT or 100 pM TGF-β1 and after 24 hours, whole-cell protein lysates were prepared in iced RIPA buffer, protein concentration determined, and 15 μg protein were subjected to immunoblotting with antibodies to collagen I, fibronectin, elastin, and α5 integrin (SDS-PAGE, 10% acrylamide). Representative immunoblot of n = 3. Panel B: eCRT but not TGF-β1, induces collagen I and Smad2 activation (Smad2P) via LRP1 signaling. HFFs, pretreated with 500 nM RAP, as described in Panel A were immunoblotted for collagen I and activated Smad2 (p-Smad2). Scanned autoradiography films were quantified using Image-J and densitometry of the wells were normalized to the corresponding intensity of β-actin compared to untreated control assigned a value of one. Representative immunoblot of n = 2. Panel C: HFFs seeded onto a 96-well plates in media containing 0.5% of FBS were treated with 50 nM, 100 nM, and 250 nM RAP or without RAP (crtl) 1 hour prior to treatment with CRT (1 and 10 ng/mL) and after 24 hours 100 μL supernatants were analyzed for TGFβ1 by ELISA according to manufacturer's instructions. RAP blocks the release of TGF-β1 induced by eCRT. Statistical significance at 1.0 ng/mL CRT comparing untreated control to pretreatment with 50 nM RAP; unpaired Student's *t* test = $P \leq .05$; *$P \leq .0206$; ⌀ $P \leq .0923$. Mean ± SD (n = 2)

(A)

MEF, 24h

(B)

MEF, 24h

(C)

MEF K42, Time course

(D)

MEF K42, 1h
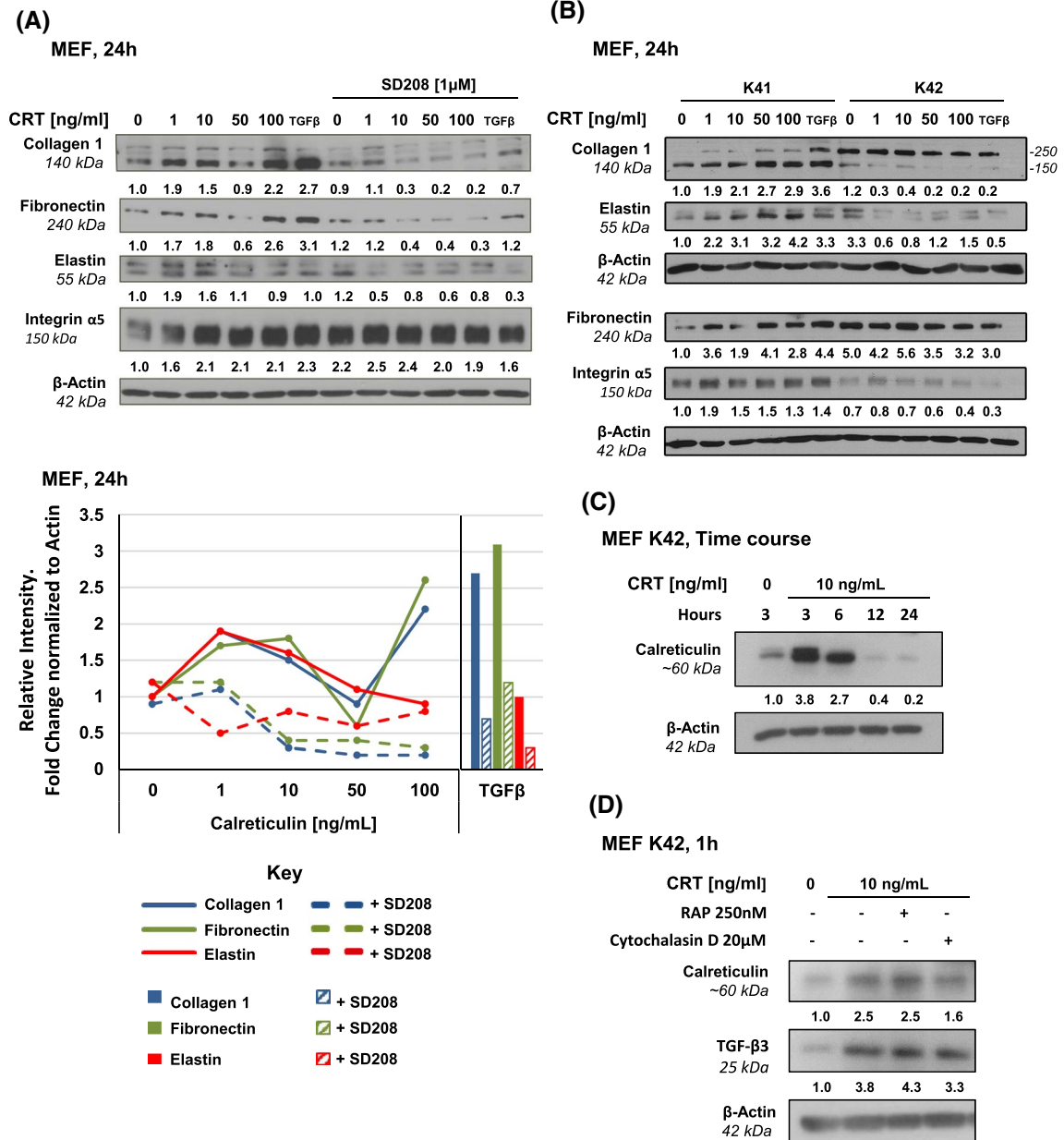
we determined whether α5 and β1 integrin induction by eCRT was likewise mediated by TGF-β signaling in HFFs and HDFs. As shown in the representative immunoblot in Figure 4A, whereas eCRT at 10 and 100 ng/mL induces a [biphasic] response in α5 integrin expression with a peak response of 1.7 and 1.4-fold, respectively, in HFFs, SD208 appeared to inhibit the eCRT-induced response at 10 ng/mL and 100 ng/mL but super-induces integrin α5 and integrin β1 in HFFs but not HDFs. eCRT similarly induced β1 integrin in HFFs, which was not blocked by SD208. In addition, a dose-dependent induction of α5 integrin by eCRT (0-100 ng/mL) was obtained in adult HDFs with a peak response of 1.6-fold at 50 ng/mL. However, the response was not inhibited by SD208 (Figure 4B). In fact, SD208 sporadically induces these integrins in HFFs and HDFs (eCRT [100 ng/mL]) compared to the untreated controls

(Figure 4A,B). Unlike the higher expression levels of ECM proteins induced by TGF-β compared to eCRT, the integrin response to TGF-β was either equal or slightly less than to eCRT in both cell lines (Figure 4A,B). Therefore, unlike the ECM proteins shown herein, the increase in α5 and β1 integrins in response to eCRT does not appear to be mediated by TGF-β signaling.

3.5 | Calreticulin increases TGF-β3 expression and release prior to ECM protein induction by human dermal fibroblasts

The data show that TGF-β canonical signaling via Smad2/3 mediates eCRT induction of collagen I, fibronectin, elastin, and α-SMA but that cross talk and other signaling

FIGURE 7 Intracellular CRT (iCRT) is required for exogenous CRT-induced ECM production, cellular proliferation, and migration of mouse embryonic fibroblasts (MEFs) but not for TGF-β3 induction; eCRT is internalized by CRT genetically null MEFS. Panel A: Similar to human fibroblasts, eCRT induces ECM proteins but not integrin α5 in mouse embryo fibroblasts (MEFs) via TGF-β1 canonical signaling. Mouse embryonic fibroblasts (MEFs) in media containing 0.5% of FBS were treated with increasing doses of eCRT (0-100 ng/mL [2000 pM]) or TGF-β1 (100 pM), in the absence or presence of the TGF-β receptor I serine/threonine kinasve inhibitor, SD208. Cell lysates were collected in iced RIPA buffer after 24 hours, protein concentration determined, and 15 μg of protein lysate subjected to immunoblotting (8% acrylamide SDS-PAGE) for collagen, fibronectin, elastin, and integrin α-5. Scanned autoradiography films were quantified using Image-Jand densitometry of the wells were normalized to the corresponding intensity of β-actin compared to untreated control assigned a value of one. Densitometric values are below each well and represented by the linear graph below the blot and adjacent bar graph for TGF-β1 effects. Representative immunoblot of n = 4. Panel B: eCRT induces collagen I, fibronectin, elastin, and integrin α5 in wild-type (K41) but CRT null (K42) MEFs were unresponsive; basal levels of the procollagen I non-cleaved precursor (259 kDa) is shown in K42 cells. K41 and K42 cells were treated with increasing doses of eCRT (0-100 ng/m/ [2000 pM]) and after 24 hours, whole-cell lysates prepared in iced RIPA buffer and equal protein concentration subjected to immunoblotting (8% acrylamide SDS-PAGE). Representative immunoblot of n = 3. Panel C: eCRT is internalized by K42 CRT null MEFS. MEFs in media containing 0.5% of FBS were treated with 10 ng/mL of eCRT, cell lysates collected in iced RIPA buffer at 3, 6, 12, and 24 hours, protein concentration determined, and 10 μg of protein lysate subjected to immunoblotting using a monoclonal antibody to human CRT (10% acrylamide SDS-PAGE). eCRT internalization occurs at 3 hours posttreatment with eCRT and is shown to decrease over time. Panel D: Internalization of eCRT and an increase in TGF-β3 following eCRT treatment in K42 CRT null MEFs occurs at 1 hour and are not mediated by LRP1 but partially blocked by Cytochalasin D. K42 MEFs were pretreated with either 250 nM RAP for 1 hour or Cytochalasin D for 30 minutes prior to addition of 10 ng/mL eCRT and cell lysates prepared 1 hour later. Unlike collagen I, fibronectin and integrin α5 (Panel B), induction of TGF-β3 by eCRT does not involve iCRT. Panel E, F: Intracellular CRT (iCRT) is partially and completely required for eCRT stimulation of migration and proliferation, respectively. Panel E: K41 wild-type and K42 CRT null MEFs were seeded in 24-well plates and migration in response to eCRT analyzed using an in vitro wound healing scratch assay (Methods). After wounding, the cells were treated with media alone or with eCRT at 1, 10, 50, and 100 ng/mL and 24 hours later, stained with 0.025% of Coomassie blue, imaged using an inverted microscope, and migration quantitated by measuring the area of the wound not covered by cells in pixels using Image-J. Quantification of wound closure (cell migration) is represented as Mean ± SD of the % of the area of the plate covered by the cells compared to the area at time 0 (n = 3). Panel F: The graph compares K41 and K42 cell migratory responses to eCRT (% migration; n = 3). *unpaired Student's t test, K41 versus K42 for CRT 10 ng/mL ($P \leq .0035$) and for CRT 100 ng/mL ($P \leq .0018$). Panel G: K41 and K42 MEFs were treated with increasing concentrations of eCRT (0-100 ng/mL) in media containing 0.5% of FBS in 96-well plates and after 48 hours, cellular proliferation was determined by the WST-8 Cell Proliferation assay. Data are represented as Mean ± SD of the % of growth compare to the untreated group (n = 3). Whereas K41 MEFs showed a dose-dependent response proliferative response to eCRT, the K42 MEFs were unresponsive (unpaired Student's t test, K41 vs K42; (*$P \leq .0000$--)

mechanisms may be involved. Therefore, we tested whether one or all of the three mammalian isoforms of TGF-β proteins are induced by eCRT, which would imply that eCRT first induces the synthesis and release of TGF-β proteins [via a separate signaling mechanism] that would subsequently signal for ECM induction [by TGF-β signaling]. Indeed, as shown in the representative immunoblot in Figure 5A, eCRT treatment of HFFs for 24 hours dose-dependently induces TGF-β1 and TGF-β3 isoforms but dose-dependently decreases TGF-β2. eCRT weakly increases transcription of all TGF-β isoforms while TGF-β1 treatment of HFFs slightly auto-induced, TGF-β3 moderately increased (3.5-fold), and TGF-β2 showing the highest transcriptional activation (8-fold)(Figure S1). By ELISA, following 24 hours treatment, eCRT at 10 ng/mL and 100 ng/mL, induces a biphasic release of TGF-β1 of 318 pg/mL and 333 pg/mL, respectively, into the culture media compared to the control of 280 pg/mL (Figure 5B; 10 ng/mL=*$P < .05$; 100 ng/mL=**$P < .01$). A TGF-β3-specific ELISA was not available to quantify the release of TGF-β3 from the CRT-treated cells.

As a mechanism involved in eCRT induction of ECM and αSMA proteins, the data suggest that TGF-β3 temporally

precedes ECM protein synthesis and release. Following seeding HFFs onto tissue culture plates, basal levels of TGF-β3 and ECM proteins, released over time to enable cell adhesion to the tissue culture plates, were determined and compared with eCRT (10 ng/mL; 200 pM) treatment. As shown in Figure 5C, whereas TGF-β3 released from untreated HFFs is observed at 3 hours, eCRT induces a 2.5-fold greater increase at this time point (arrows). In untreated cells, release of basal levels of collagen I and fibronectin are observed at 6 and 24 hours, respectively. However, eCRT induces a greater release of both proteins commencing at 3 hours with fibronectin continuing to be released at high levels through 48 hours and collagen waning between 18 and 24 hours. In addition, low basal levels of elastin are observed at 3 hours, induced 2.6-fold by eCRT at this time point, and are maintained at this level until 48 hours when basal levels are again observed.

Since TGF-β3 release is observed at an earlier time point than the ECM proteins, except low basal levels of elastin are consistently observed, a time course of eCRT (10 ng/mL;200 pM) induction of the synthesis of ECM proteins and TGF-β1 and TGF-β3 was performed in HFFs. Figure 5D
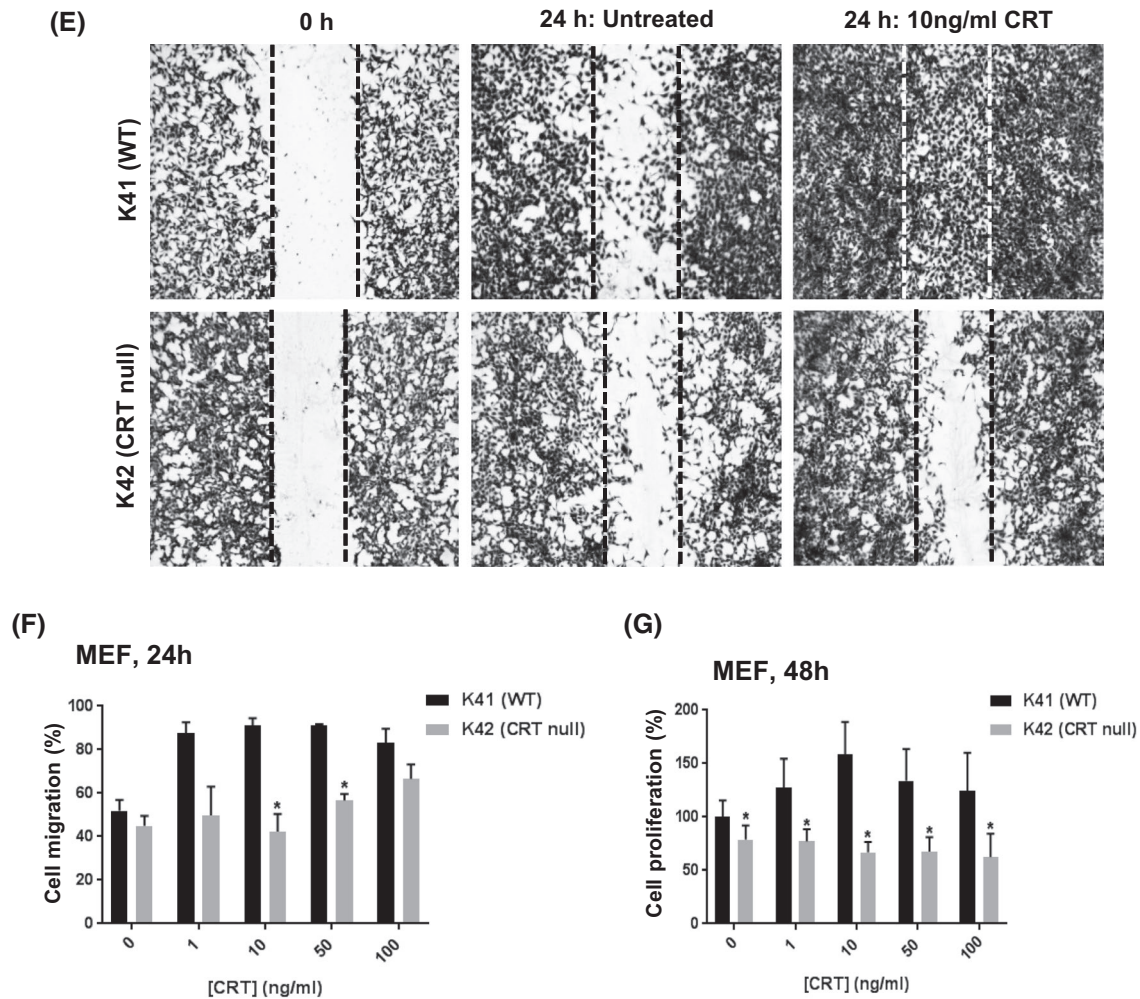
FIGURE 7 Continued

shows that in cell lysates, TGF-β1 is constitutively produced and that CRT (10 ng/mL [200 pM]) induces synthesis of TGF-β3 protein at 6.8-fold over the basal level at 3 hours in this representative immunoblot. Therefore, the stimulation of the synthesis of TGF-β3 is earlier than collagen I and elastin shown at 6 hours (1.76-fold and 1.64-fold, respectively [compare untreated to CRT at 10 ng/mL at each time point]). eCRT also induces fibronectin at this early time point but, as shown in Figure 3A, at 24 hours this appears to be mediated by TGF-β signaling. Thus, the induction of fibronectin by eCRT at 3 hours suggests non-TGF-β-mediated signaling earlier and TGF-β signaling during later time points. Irrespective of eCRT induced effects on ECM proteins, a separate experiment shows basal levels of fibronectin and elastin over time exemplifying the erratic and possibly cyclic synthesis of these proteins as the cells respond to adhesion requirements for survival (Figure S2). It is notable in Figure 5D that eCRT collagen, fibronectin, elastin, TGF-β1, and TGF-β3 dissipate and are no longer induced by eCRT at 48 hours post-treatment.

3.6 | Induction of TGFβ1 release and extracellular matrix protein induction by exogenous calreticulin but not by exogenous TGF-β1 is mediated by LDL Receptor-Related Protein-1 (LRP1)

Herein, we show that eCRT induction of ECM proteins is mediated with varied dependencies through TGF-β canonical signaling and that temporally, TGF-β3 is ostensibly synthesized and released from fibroblasts prior to ECM protein induction and release (Figure 5C,D). Cell surface CRT has been shown to associate with the LRP1/CD91 receptor for functional signaling to elicit cellular responses.[2,34,62-65] It is notable that to date, the LRP1 in a complex with different accessory proteins, such as thrombospondin 1, is the only signaling receptor shown to mediate exogenous/extracellular CRT-induced activities.[2,7] Therefore, to determine whether LRP1 is a receptor that initially responds to CRT for subsequent downstream signaling through TGF-β canonical signaling and other signaling mechanisms for ECM
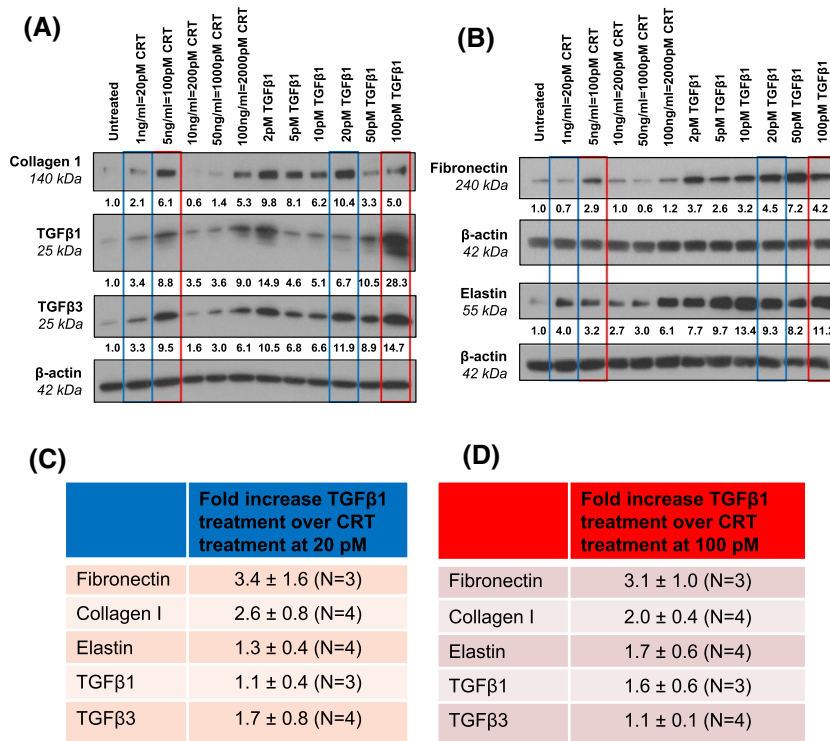
FIGURE 8   By molar comparison, exogenous calreticulin is less potent than TGF-β1 in induction of ECM proteins. HFFs were treated with increasing doses of eCRT (20 pM to 2000 pM or TGF-β1 (2 pM to 100 pM) in media containing 0.5% of FBS. After 24 hours cell protein lysates were prepared in RIPA buffer, protein concentrations determined and 10-20 μg of cell lysate applied to well of a 10% of SDS-PAGE. Proteins were transferred to nitrocellulose membranes and immunoblotted for collagen I, fibronectin, elastin, TGF-β1, and TGF-β3 followed by autoradiography and densitometric scanning of each lane to determine the protein levels in each well normalized to β-actin and compared to untreated controls assigned a value of one; values were quantified using image-J. (A,) The intensity of ECM protein bands and TGF-β1 and TGF-β3 for the treatments of 20 pM eCRT and TGF-β1 are highlighted with a blue rectangle and for (B) 100 pM eCRT and TGF-β1 are highlighted with a red rectangle. Fold-induction when comparing levels of each protein for 20 pM TGF-β1 vs eCRT treatments (C) Blue left table) and for 100 pM TGFβ1 vs eCRT treatments (D) Red right table) are shown as Mean ± SD values from densitometry values comprising 3-4 experiments

and integrin α5 induction, HFFs were pretreated with the LRP inhibitor, receptor associated protein (RAP), which titrates out LRP signaling.[66] In a representative experiment, Figure 6A,B shows that 250 nm and 500 nM RAP partially blocks eCRT induction of collagen I, fibronectin, and elastin (Figure 6A). However, fibronectin was more fully blocked (80%) with the lower concentration of RAP. In contrast, blocking LRP1 signaling did not affect eCRT induction of integrin α5. These data suggest that eCRT binds to LRP1 to induce the ECM proteins tested here but that a different receptor mediates the induction of integrin α5 in HFFs by eCRT. Similar to the data using the TβRI kinase inhibitor, SD208 (Figure 3), the treatment of HFFs with 500 nM RAP super-induced collagen I and elastin. However, these proteins were induced by eCRT to a greater extent than by RAP and, were clearly inhibited by RAP. Importantly, TGF-β induction of ECM proteins was clearly not inhibited

by RAP (Figure 6A) and as shown in Figure 6B, RAP did not inhibit activation/phosphorylation of Smad2 or again, collagen induction by TGF-β. However, RAP blocked the eCRT-induced increase in collagen by 60% but not TGF-β1 (Figure 6B) induction of collagen. As shown in Figure 6C, as measured by ELISA, RAP dose-dependently inhibited eCRT-induced release of TGFβ1 from HFFs, which was statistically significant at 1 ng/mL eCRT with a trend shown at 10 ng/mL. Taken together, the data suggest that eCRT induces TGF-β synthesis and release in part, by binding to an LRP receptor, likely LRP1, and the release of TGF-β subsequently signals via classic canonical TGF-β-Smad2/3 signaling to induce ECM proteins and α-SMA. However, the induction of collagen I and elastin by RAP, the super-induction of elastin by TGF-β in presence of RAP, and the inhibition by RAP of fibronectin at lower concentrations do not allow for unequivocal conclusions.
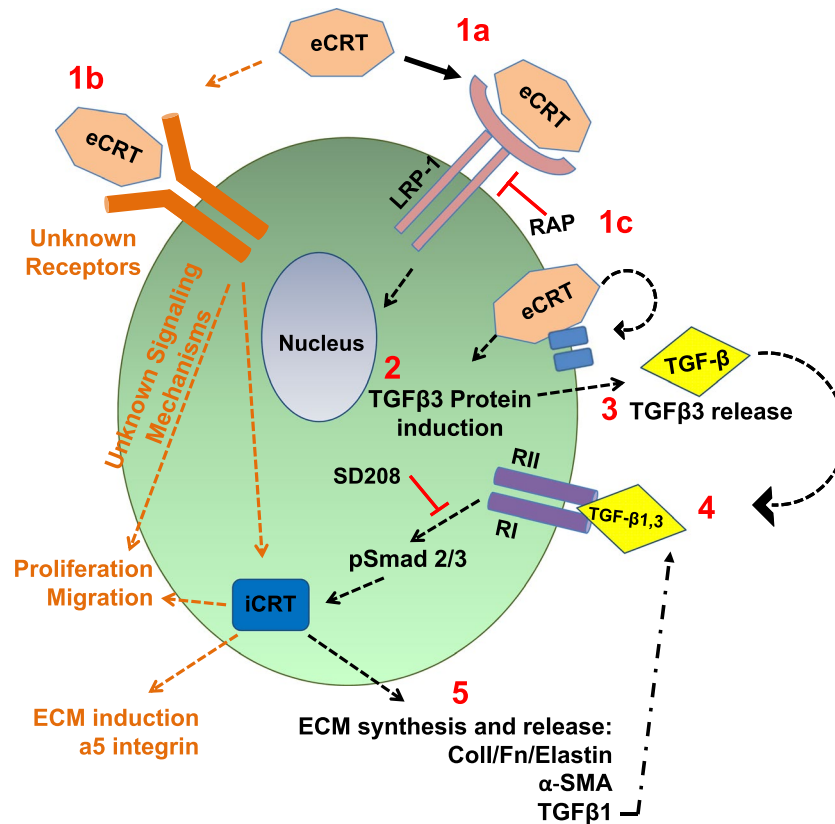
FIGURE 9 Exogenous [extracellular] CRT induces collagen I, fibronectin, elastin, and α-smooth muscle actin by LRP1 binding and downstream TGF-β canonical signaling, and otherunidentified [signaling] mechanisms. The diagram depicts a simplified version of eCRT outside-in signaling with the following schema: *(1a) eCRT (orange hexagon) binds to an LRP receptor, possibly LRP1 (pink receptor) [inhibited by RAP][2] initiating a cascade of uncharacterized intracellular signaling event(s) that elicits the release of TGF-β3[3] isoform (yellow diamond) by 3 hours and subsequently, by binding and activating the TGF-β receptor complex (RII, RI) (purple receptor) and downstream activation of TGF-β transcription factors, pSmad2/3 [inhibited by SD208 TβRI ser/thr kinase inhibitor][4] to induce the synthesis and release of the ECM proteins collagen I, fibronectin, elastin, αSMA, and TGF-β1.[5] The constitutive expression and release of TGF-β1 continues to promote TGF-β canonical signaling contributing to the production of these proteins (dashed and dotted line). However, the induction of ECM proteins and αSMA by eCRT is variably dependent on TGF-β1 and TGF-β3 signaling via binding to TRβII followed by TRβI (purple) canonical downstream Smad2/3 signaling [inhibited by SD208]. *(1b) Extracellular matrix proteins might be directly induced by LRP1 and/or other receptor signaling pathways (orange receptor and orange intracellular intermediate signaling pathways). Experiments using CRT null MEFs show the requirement for intracellular CRT (iCRT) (blue box) in eCRT-dependent collagen, fibronectin (Fn), elastin, αSMA, integrin α5 induction, cell proliferation, and in part, cell migration. Therefore, eCRT and iCRT converge to enable functions important in wound healing. *(1c) In K42 CRT null MEFS, eCRT is internalized by 1 hour in part by an endocytic and non-endocytic [receptor] mechanism (blue receptor), and subsequently degraded by 12 hours; internalized eCRT might signal to induce ECM proteins and TGF-β3, which is shown to increase in 1 hour in a LRP1-independent manner. The data show a complex process and open many avenues for investigation. The induction of TGF-β3 in 1 hour does not require iCRT but results might be different in human fibroblasts and at later time points after eCRT treatment

3.7 | Intracellular CRT (iCRT) is required for extracellular/exogenous CRT (eCRT)-induced ECM production, cellular proliferation and in part, migration of fibroblasts but not for eCRT early induction of TGF-β3

CRT plays a significant role in collagen I expression, chaperoning through the ER, and processing to the fibrillar form for extracellular matrix formation.[6] CRT null mouse embryo fibroblasts (K42 cells; MEFs) have reduced collagen and fibronectin matrix formation compared to wild-type

(WT) MEFs (K41 cells), which leads to a reduction in adhesion.[67] Furthermore, using K42 cells, it was shown that TGF-β induction of mature collagen type I and fibronectin required intracellular CRT (iCRT).[5] Therefore, since we show herein that the induction of ECM proteins by eCRT in human fibroblasts is largely mediated by TGF-β canonical signaling [downstream from LRP1 signaling], the dependence or connection between iCRT and eCRT in the induction of ECM proteins was investigated comparing mouse CRT null K42 cells with wild-type, K41 cells. First, similar to HDFs and HFFs, in the representative immunoblot shown in Figure 7A, eCRT (0-100 ng/mL) treatment of K41 MEFs

induces a biphasic response in the levels of collagen I, fibronectin, and elastin proteins (1.6-2.6-fold), which were inhibited by SD208. In contrast, similar to the response obtained with human fibroblasts, α5 integrin is induced but not inhibited by SD208. The mouse fibroblasts responded with similar levels of ECM proteins to both 100 pM TGF-β and 2000 pM eCRT (100 ng/mL). Therefore, similar to the response of human fibroblasts, TGF-β is 20 times more potent than eCRT in induction of ECM proteins in MEFs. As shown in Figure 7B, whereas eCRT induces synthesis of collagen I, fibronectin, elastin, and integrin α5 in the WT K41 MEFs, none of these proteins were induced in the K42 CRT null MEFs. Unprocessed collagen I precursor was shown at 250 KDa in the K42 cells with both eCRT and TGF-β treatment and increasing doses of eCRT appeared to reduce this precursor form of collagen. Whereas five times more basal levels of fibronectin protein are synthesized by the CRT null MEF K42 cells than the wild-type K41 MEFs, the cells were unresponsive to eCRT. In addition, only a very low basal level of α5 integrin is produced in the K42 CRT null cells, which is not induced by eCRT.

We exploited the lack of CRT in K42 MEFs to determine whether exogenously added CRT could be internalized over time by immunoblotting using an antibody to human CRT. A low level of CRT in the CRT null cells was detected by the antibody, which might be due to CRT derived from the FBS that had accumulated on the surface of the cells. By the immunoblot shown in Figure 7C, eCRT added to K42 cells appears to be internalized with an increase of 3.8-fold in the cell lysates by 3 hours, which decreases at 6 hours to 2.7-fold dissipating by 12 and 24 hours (Figure 7C). Alternatively, it cannot be excluded that eCRT was detected because of binding the cell surface of the K42 cells that is released or degraded on the cell surface overtime. Since as shown in Figure 7D, RAP did not inhibit eCRT detection in cell lysates, eCRT was not internalized via LRP1 binding. More likely, eCRT was internalized by the K42 cells, in part, by an endocytic/macropinocytotic mechanism since cytochalasin D partially decreased (by 36%) the amount of eCRT detected (Figure 7D). In addition, Figure 7D shows that TGF-β3 protein is induced within 1 hour in CRT null K42 cells, which is not inhibited by RAP but was partially inhibited by cytochalasin D. Therefore, unlike ECM proteins and integrin α5, the induction of TGF-β3, in CRT null cells does not require iCRT and a receptor other than LRP1 signals downstream gene targets of TGF-β3.

In vitro activities of eCRT, reported using human fibroblasts, are consistent with the role for topical [exogenous] CRT in enhancing the rate and quality of wound healing thereby underscoring the mechanisms of action of this chaperone protein in wound repair.[22-24,68] Specifically, in addition to ECM induction shown herein, in vitro, eCRT induced concentration-dependent migration in a chamber assay, motility

in a scratch plate in vitro wound healing assay, and stimulated proliferation of human and mouse fibroblasts. As we show that iCRT is required for ECM and α5 integrin induction by eCRT, to determine whether iCRT is similarly required for eCRT induction of fibroblast migration and proliferation, we performed migration and cellular proliferation assays, as previously described,[22] using K41 WT and K42 CRT null⁻ MEFs. Whereas both the wild-type K41 and K42 CRT null cells showed similar closure of the in vitro wound with the higher concentration of CRT at 100 ng/mL (Figure 7E,F) the wild-type K41 MEFs showed 83%-91% closure of the scratch wound at a threshold concentration of 1.0-100 ng/mL. Thus, the K42 CRT null MEFs were 10 times less sensitive to eCRT than the K41 WT MEFs (compare eCRT 10 ng/mL in K41 cells [top panel] to K42 cells [bottom panel] (Figure 7E), which was statistically significant at 10 ng/mL ($P \leq .0035$) and 50 ng/mL ($P \leq .0018$). (Figure 7F). In addition, whereas the K41 WT cells show a dose-dependent proliferative response to CRT that peaked at 10 ng/mL (1.5-fold over control), the K42 CRT null cells were unresponsive (Figure 7G). Therefore, similar to eCRT-induction of ECM proteins and α5 integrin, cellular proliferation requires intracellular [chaperone] CRT (iCRT) and cell migration was blunted in the absence of iCRT.

3.8 | Calreticulin is less potent in induction of ECM proteins than TGF-β1

As noted herein (Figures 2, 3, and 7), eCRT at 2-20 times the molar concentration of TGF-β1 induced a lower induction of ECM proteins. Therefore, to compare the potency between eCRT [which as shown herein induces TGF-β1 and TGF-β3] and TGF-β on ECM and TGF-β1 and TGF-β3 protein expression, HFFs were treated with increasing concentrations of eCRT and TGF-β1 for 24 hours and the level of ECM, TGF-β1, and TGF-β3 protein expression analyzed. The representative immunoblots in Figure 8A show that at equimolar comparisons of eCRT and TGF-β, eCRT treatment of HFFs resulted in lower induction of the target proteins. The differences are highly notable by the boxes drawn for comparison of eCRT vs TGF-β at 20 (blue) and 100 pM (red) on the blots. Collagen I and fibronectin induction were more disparate in their responses than TGF-β1 and TGF-β3. Panel C (Table) of the densitometry values from four immunoblots shows the fold increase of TGF-β treatment over eCRT at 20 pM (blue outline) and in Panel D (Table) at 100 pM (red outline). At both concentrations, a similar fold difference was observed. At 20 pM and 100 pM, TGF-β1 compared to eCRT induced an average 3.4 and 3.1-fold increase in fibronectin, a 2.6 and 2.0-fold increase in collagen I, a 1.3 and 1.7 increase in elastin, a 1.1 and 1.6 increase in TGF-β1, and a 1.5 and 1.1 increase

in TGF-β3, respectively, at 24 hours. The differences in induction of collagen and fibronectin by TGF-β were more robust than for elastin, TGF-β1, and TGF-β3. Therefore, on a molar basis, TGF-β, known to contribute to cutaneous scarring due to dysregulated ECM protein synthesis induces 1.7-3.4 fold more ECM proteins by human fibroblasts in vitro than eCRT, which heals wounds by a tissue regenerative process without scarring.[22]

4 | DISCUSSION

Following topical application of CRT to full-thickness excisional wounds on the dorsum of diabetic mice, abundant granulation tissue formation was observed within 3 days post-wounding compared to scant amounts in buffer-treated wounds. Consistent with the abundant granulation tissue at this early time post-wounding, the CRT treated wounds expressed high levels of procollagen I and fibronectin compared to scant amounts in the buffer treated diabetic mouse wounds. By day 28 post injury, the presence of epidermal appendages in the CRT treated wound compared to buffer treatment implicates that CRT induced a tissue regenerative process during wound repair. Recapitulating the in vivo results and compared with TGF-β as a well-known inducer of ECM proteins (positive control), we show, in vitro, that eCRT dose-dependently induces collagen I, fibronectin, and elastin synthesis by human fibroblasts, which was completely or partially blocked by chemical inhibition of TGF-β RI kinase activity with SD208. Moreover, the studies show that the induction of ECM proteins by eCRT was deficient in CRT null mice. Therefore, eCRT outside-in signaling induces ECM proteins and α-SMA that is mediated by TGF-β canonical signaling requiring iCRT. However, whereas SD208 completely blocked TGF-β signaling particularly, eCRT stimulation of elastin was not completely blocked in HFFs and HDFs. As RAP, the LRP1 antagonist,[64] inhibited eCRT but not TGF-β stimulation of ECM proteins or activation of the downstream transcription factor for TGF-β targeted genes, Smad2P, LRP1 might directly signal through accessory proteins or different intermediate pathways other than TGF-β signaling for ECM protein induction. Moreover, whereas we show that LRP1 and TGF-β are involved in eCRT induction of ECM proteins, their interaction is unclear. Consistent with TGF-β canonical signaling, both Smad2 and Smad3, were activated by eCRT and blocked by SD208. Particularly, Smad3 activation has been associated with TGF-β-mediated fibrosis specifically apparent in systemic scleroderma and pulmonary fibrosis[37,69,70] and is essential for the activation of most fibrillar collagen genes. Furthermore, Smad3 null mice are protected against radiation-induced fibrosis of the skin.[71] It is notable that

treatment with SD208-induced ECM proteins above basal levels without the addition of eCRT in neonatal HFFs but not adult HDFs and further, super-induced elastin levels over eCRT doses in both cell lines. This increase in protein synthesis might reflect a rebound or positive feedback loop in an effort by the cells to maintain adherence to the tissue culture plate in the presence of blocking TGF-β receptor signaling needed for ECM substrate induction for cell adhesion. The super-induction of collagen by SD208 prevented a clear conclusion regarding the extent of TGF-β signaling for eCRT induction of collagen. Whereas ECM and α-SMA protein induction by eCRT was generally robust, mRNA levels were consistently below 2-fold and not statistically significant. Similar to ECM protein induction, TGF-β induced a higher level of transcription of collagen and fibronectin than eCRT. Further studies, such as ribosome profiling are important to determine mechanisms involved in the discordant low levels of mRNA of ECM proteins induced by eCRT; low transcription levels of these mRNAs has been shown by others.[6,8,72] Preliminary studies using cycloheximide suggest that there is a rapid rate of translation of ECM proteins following eCRT treatment of HFFs (unpublished results) suggesting a rapid rate of mRNA turn-over.

Cell surface integrin receptors consist of heterodimers of transmembrane alpha and beta subunits. Following activation, integrins signal to enable cell adhesion, migration, ECM assembly and growth factor signaling, and are thus, essential to all phases of wound healing particularly, granulation tissue formation critical to construct the neodermis in wound repair.[73,74] We show that eCRT dose-dependently increases alpha 5 and beta 1 integrin expression by human fibroblasts. However, unlike the ECM proteins and α-SMA, induction of these integrins was not mediated by TβRI signaling in human fibroblasts. Again, SD208 super induced both integrins at different concentrations, and thus, these data are not conclusive. Moreover, TGF-β stimulation of alpha 5 was slight or within background levels, whereas induction of ECM proteins by TGF-β on a molar basis was higher at 1.3-3.4-fold greater than eCRT (Figure 8). eCRT induction of both α5β1 integrins and fibronectin may play a role in the mechanism of fibroblasts migration into the wound and also, keratinocyte migration from the epithelial tongues on fibronectin substrate located under the eschar to enable wound closure.[75] In terms of lack of scarring observed in mouse wounds treated with eCRT, the interaction of the fibroblast cell surface α5β1 integrin with fibronectin and fibronectin binding to collagen via its collagen binding domain is important for proper collagen fibril formation and organization (non-scarring)[76-78] eCRT might act through induction of integrins and fibronectin for the observed anti-scarring effect shown in mouse excisional wounds.[22] Interestingly, rotary jet spinning of fibronectin

into nanofibers, that mimicked the non-scarring fibronectin fibrillogenesis found in fetal skin, was shown to accelerate wound closure with a tissue regenerative phenotype.[79]

Time course experiments show that prior to ECM induction, eCRT specifically induces TGF-β3, which was both secreted into the culture media and observed in cell lysates of HFFs at 3 hours post-treatment. Basal levels of TGF-β1, collagen, fibronectin, and elastin were shown in cell lysates at 3 hours but were not induced by eCRT until 6 hours for collagen and elastin and 12 hours for fibronectin and TGF-β1. The temporal cyclical expression of basal levels of elastin and fibronectin shown in Figure S2 is consistent with cell signaling negative and positive feedback loops producing substratum during dynamic adherence and cell migration. Despite rigorous control over cell density, timing of experiments, and consistent cell passage numbers, it appears that the adhesion requirement of the cells has interfered with a clear and consistent assessment of the induction of ECM proteins by eCRT and experimental variability was difficult to control. However, taken together, eCRT clearly induces ECM proteins via TGF-β signaling and likely other signaling pathways or mechanisms and appropriately, collagen and fibronectin are shown in cell lysates prior to their secretion into the media (Figure 5C,D).

Whereas in vitro [at 24 hours], eCRT induced both TGFβ1 and TGF-β3, in vivo, TGF-β3, but not the other isoforms, was increased in the dermis following CRT topical treatment murine and porcine wounds.[23] Specifically, TGF-β3 has been shown to regulate migration of epidermal and dermal cells in injured skin.[80] Whereas auto-induction and cross-induction of TGFβ isoforms has been shown,[81] TGF-β2 was decreased by eCRT in HFFs. As differential functions and localization of TGFβ isoforms are known,[52] it is possible that the presence of TGF-β2 is counterproductive to the tissue regenerative response of fibroblasts to eCRT. This is consistent with the lack of TGF-β2 in vivo in the wound tissues treated with CRT.[22,23] Notably, eCRT induction of TGFβ3 occurred earlier than its effect on TGF-β1. Furthermore, whereas both TGF-β1 and TGF-β2 promote fibrosis,[40,82] TGF-β3 is associated with anti-fibrotic responses in certain tissues[83] and in human clinical trials, TGF-β3 improved scarring of full-thickness excisional wounds.[84] Our data suggest that the induction of TGF-β3 by eCRT might shift wound healing toward an anti-fibrotic response. Another notable observation is that between 18 and 48 hours, fibronectin, collagen, elastin, TGF-β3, and TGF-β1 less so, were no longer induced by CRT suggesting a mechanism of dampening eCRT induction of ECM proteins following peak responses. This is an intriguing possibility to explain CRT-induction of tissue regeneration vs TGF-β promotion of scarring, as shown in vivo following excisional wounding of diabetic mice.[22]

CRT is localized to the cell surface of numerous cell types including fibroblasts, endothelial cells, platelets, and apoptotic cells but it does not have transmembrane signaling function.[2] As the low-density lipoprotein (LDL)-receptor related protein 1 (LRP1) is the only consistently demonstrated cell surface signaling receptor for eCRT-mediated effects, we evaluated LRP1 as the upstream receptor that binds to exogenous CRT.[7,34,63,85] LRP1, composed of a 515 kDa alpha chain and 85 kDa beta chain, broadly binds to 35 physically and functionally unrelated ligands with high affinity.[86] Receptor associated protein (RAP), a molecular chaperone that binds LRP1 and other members of the lipoprotein receptor family, trafficks these receptors to the Golgi where the complex is dissociated.[87] Interestingly, exogenous RAP is a highly potent antagonist of LRP1 ligand binding, and thus, LRP cell surface receptor signaling. Our data show that 500 nM RAP blocked eCRT induction of collagen in HFFs. In contrast, both elastin and α5 integrin induction by eCRT were not inhibited by RAP and in fact, this protein inhibitor appeared to have agonistic activity for integrin α5. Notably, the binding of RAP to LRP1 without eCRT exerted a 2-fold agonistic effect on collagen induction. Therefore, whereas (a) different receptor(s) might signal for CRT stimulation of elastin and α5 integrin, the apparent agonistic effect of RAP binding to LRP1 confounded the ability to detect eCRT-induced LRP-1 signaling for synthesis of these two proteins. In addition, RAP dose-dependently blocked eCRT-induced TGF-β1 release from the cells. RAP did not block TGF-β1 direct induction of collagen or fibronectin but unexplainably, super-induced TGF-β1 induction of elastin. TGF-β1 has been shown to bind directly to LRP1 by others,[88,89] particularly in the context of growth regulation function. However, at least for ECM induction, according to our studies herein, TGF-β1 binding to LRP1 is not apparently involved in eCRT induction of ECM in HFFs. Whereas LRP1 signaling, blocked by RAP, inhibited CRT-induced fibronectin and collagen implicating LRP1 in CRT signaling, a more precise unraveling of other receptors for CRT signaling needs further investigation. Other receptors including scavenger receptor-1 Sca-1 in the context of CRT-induced cytokine release by macrophages and endocytic mechanisms for signaling have been shown.[36,90,91]

Similar to HFFs and HDFs, eCRT induction of ECM proteins, but not α5 integrin in mouse embryo fibroblasts (MEFs) is mediated by TGF-β signaling. The TGF-β-mediated fibrotic response involves regulation by iCRT[5] as CRT null mice and lung fibroblasts from idiopathic pulmonary fibrosis with siRNA CRT knockdown compared to wild-type and non-transfected cells, showed defects in both collagen and fibronectin protein production in response to TGF-β with Smad2/3 activation remaining intact. Accordingly, CRT null MEFs (K42) are less adherent than wild-type MEFs of the same murine strain (K41),[92] express lower levels of fibronectin,[93,94] show differences in metalloproteinase expression[95] and the lack of cytoplasmic CRT obviates its function in stabilizing integrin-mediated adhesion to collagen via CRT

binding to the cytoplasmic tail of the integrin α subunit.[31,96,97] Conversely, the overexpression of CRT in fibroblasts is consistent with higher fibronectin mRNA and protein, increased collagen I (*Col1A2*) and greater deposition of ECM.[93,94] Similar results as previously shown for CRT null MEFs,[6] were obtained herein by comparing the effect of eCRT on ECM protein induction. CRT null MEFs treated with eCRT only produced the uncleaved procollagen I precursor and collagen was not induced by eCRT compared to wild-type MEFs. These results replicate the characteristics of null CRT cells expressing increased basal levels of procollagen I, which remains unprocessed, bound to iCRT, and retained in the ER.[6] The CRT null K42 MEFs expressed five times higher levels of fibronectin than the wild-type. However, again, these cells were unresponsive to eCRT in increasing fibronectin levels. Conversely, the induction of TGF-β3 by eCRT within 1 hour did not require iCRT. Thus, whereas eCRT induction of collagen I and fibronectin by TGF-β require iCRT, at least the TGF-β3 isoform can be induced by eCRT in K42 cells thereby raising more questions regarding the interaction and cross talk of TGF-β3 and iCRT in fibrosis. Furthermore, eCRT appears to be internalized by K42 MEFs as shown by 1 and 3 hours post-addition. Since eCRT internalization was not inhibited by RAP but was partially inhibited by cytochalasin D, eCRT is not internalized through LRP1 binding but at least in part, is mediated by an endocytic mechanism apparently involving intracellular endosomal degradation as the level of eCRT dissipates at 6 hours and disappears by 12 hours. However, prior to 6 hours, eCRT might signal or interact with intermediate signaling mechanisms by endosomal escape. The binding of eCRT to the cell surface and its entry into the cell, which might involve direct translocation through the membrane and/or any endocytic mechanism including macropinocytosis, clathrin, or caveolae-mediated endocytosis[98] warrants further investigation using specific inhibitors. These experiments elucidate new pathways for further analysis of the mechanism of eCRT cell surface binding for cell entry and its downstream effects. However, since these studies were performed in CRT null mouse fibroblasts, whether exogenously added CRT is internalized by human fibroblasts and is a mechanism of eCRT signaling also, should be further investigated. The connection between eCRT internalization as a mean for ECM induction could not be queried since iCRT is shown herein to be required for ECM and integrin α5 induction. The rapid increase in TGF-β3 observed at 1 hour following addition of eCRT was not through LRP1 binding [not inhibited by RAP] but ostensibly in part involved a type of endocytic/pinocytotic uptake mechanism [partially inhibited by Cytochalasin D] and in part, binding of eCRT to an unknown cell surface receptor. This early, within 1 hour upregulation of TGF-β3 by eCRT in CRT null cells, does not involve LRP1 and yet, we show that LRP1 mediates eCRT induction of ECM proteins via TGF-β

canonical signaling. This complicates the role for TGF-β3 release within 3 hours being involved in signaling for ECM induction through binding to the TGF-β receptor complex (RI and RII)/Smad2/3 activation. Nonetheless, TGF-β3 signaling early through a different receptor (non-LRP1) might initiate a separate set of downstream proteins from ECM proteins. Since the experiments using RAP to implicate LRP1 signaling by eCRT were performed in a 24 hour window both the TGF-β1 and TGF-β3 released have the potential to bind to TGF-β receptor complex for eCRT-induced ECM induction mediated by these TGF-β isoforms. Clearly, the mechanisms involved in eCRT induction of ECM protein through LRP1 and interactions evoking TGF-β receptor signaling are complex as shown by the data presented herein in which cell-type and temporal responses influence outcomes. Thus, the current studies raise a plethora of questions that when answered should shed light on cellular processes involved in fibrosis.

In direct contrast to our results shown here, exogenously added CRT did not increase soluble collagen production in wild-type MEFs.[6] This is inconsistent with our results in vivo showing that topical CRT increases collagen I deposition in murine and porcine wounds.[22,23] In addition, experimental conditions between these studies were disparate as we added doses of 1.0 to 100 ng/mL (2000 pM) to the cells, whereas Graham et al,[6] treated CRT null K42 and K41 wild-type MEFs with 1.0 μM eCRT (0.5×10^8 more eCRT). As we show that higher doses of eCRT can decrease ECM proteins, this high dose of eCRT might have quelled receptor signaling/cycling by negative feedback thereby muting the collagen response. Nonetheless, our data shows a unique requirement for iCRT in the level of induction of fibronectin and collagen processing by eCRT.

In CRT wild-type K41 MEFs, moderate levels of α5 integrin were expressed. In contrast, α5 integrin was barely expressed in the CRT null MEFs and eCRT did not elicit a response. The important role of α5 integrin in sensing the ECM and modifying cellular responses, such as in matrix remodeling and wound repair, suggests that CRT null cells have a deficiency in tissue remodeling. Notably, CRT is a critical chaperone for integrins in the ER and in the cytoplasm, CRT physically binds to the KxGFFFKR amino acid sequence in the cytoplasmic tails of α-integrins for activation of FAK involved in cell intermediate adhesion related to cell migration.[2,62,64,96,99] With respect to intracellular CRT functions in other aspects of wound healing besides induction of ECM proteins and integrins, we show that CRT null cells did not respond to eCRT for stimulation of proliferation and the eCRT-induced migratory response was blunted. iCRT might be required for the chaperoning of proteins required for proliferation and migration or in mechanisms related to these functions, such as effects on the cytoskeleton.[7,64,100] Nonetheless, it is most interesting that intracellular and extracellular CRT converge on implementing many functional

responses involved in the pathological fibrotic response and physiological wound healing, which impact the molecular level cell functional processes that underscore these systemic responses.

The diagram in Figure 9 depicts a series of signaling events gleaned from our studies that are involved in eCRT induction of ECM proteins, αSMA, and α5 integrin. Although the data implicate that other signaling mechanisms are involved, CRT signaling via LRP1 induces collagen, fibronectin elastin, and α-SMA by the synthesis and release of TGF-β3 (and possibly TGF-β1). TGF-βs bind and activate TGF-β receptor signaling thereby initiating Smad2/3 signaling for transcription of ECM genes and TGF-β1, requiring iCRT for ECM protein trafficking, processing, and release. Other TGF-β-mediated functions have been shown to require iCRT. For example, unlike their wild-type counterparts, CRT null stem cells from embryoid bodies are unable to respond to TGF-β in the induction of epithelial to mesenchymal transition (EMT), a process required for cardiomyogenesis[101] involving TGF-β regulation of the e-cadherin switch and upregulation of Snail2/Slug during EMT. These studies showed that calcium-mediated signaling via iCRT interaction with calcineurin, the Wnt pathway, and TGF-β canonical and noncanonical signaling was involved. Thus, this is consistent with the requirement for iCRT for ECM induction and, for EMT as a mechanism for cardiac stem cell differentiation. Whereas studies to date exploited CRT null cells to show the involvement of iCRT in TGF-β-mediated functions and moreover,[2,3,6,64,101-103] all these studies utilized CRT null cells to obviate the function of CRT in scarring, the experiments described here are the first to show an eCRT- iCRT co-dependency in the mediation of CRT-induced functions through outside-in signaling largely involving TGF-β signaling. It is possible that eCRT signaling exerts cellular actions that changes or counters the course of the role of iCRT in fibrosis and scarring by quelling this dynamic process.

Harnessing the fibrotic response to ensure that outcomes from tissue injury terminate in tissue regeneration is a medically important goal. CRT is the first topically applied biotherapeutic that exhibits tissue regenerative characteristics, as we have shown for excisional wounds in diabetic mice.[22,24] Organ fibrosis causing loss of function and death contrasts directly with functional tissue regeneration. Our data suggest that, despite acting via TGF-β signaling to promote ECM production, CRT modulates and mitigates the TGF-β fibrotic response, as exemplified here, by inducing lower levels of ECM proteins. Since repair of fetal wounds early in gestation heal by a tissue regenerative process without scarring, we envision that eCRT might exploit certain mechanisms operative during fetal tissue (re)-generation. Revealing the mechanisms and pathways involved in CRT-driven tissue repair should implicate molecular targets to affect healing of both acute and chronic wounds by tissue bioengineering.

CONFLICT OF INTEREST

L. I. Gold discloses that she has a financial interest including stock ownership and an advisory role in Tissue Regeneration Sciences, Inc This company is developing calreticulin for tissue regeneration and reconstruction for different medical indications. All other authors have no declarations of interest, acknowledgments, and disclosures of financial and material support.

AUTHOR CONTRIBUTIONS

L. Gold designed research, analyzed data, and wrote the paper; A. Tellechea performed research, analyzed data, and wrote the paper; U.M. Pandya, M.A. Manzanares, C. Egbuta, C. Jimenez Jaramillo, F. Samra, A. Fredston-Hermann, and K. Saadipour performed research and analyzed data.

REFERENCES

1. Michalak M, Groenendyk J, Szabo E, Gold LI, Opas M. Calreticulin, a multi-process calcium-buffering chaperone of the endoplasmic reticulum. *Biochem J*. 2009;417:651-666.
2. Gold LI, Eggleton P, Sweetwyne MT, et al. Calreticulin: non-endoplasmic reticulum functions in physiology and disease. *FASEB J*. 2010;24:665-683.
3. Gold L, Williams D, Groenendyk J, Michalak M, Eggleton P. Unfolding the complexities of ER chaperones in health and disease: report on the 11th international calreticulin workshop. *Cell Stress Chaperones*. 2015;20:875-883.
4. Groenendyk J, Lynch J, Michalak M. Calreticulin, Ca2+, and calcineurin—signaling from the endoplasmic reticulum. *Mol Cells*. 2004;17:383-389.
5. Zimmerman KA, Graham LV, Pallero MA, Murphy-Ullrich JE. Calreticulin regulates transforming growth factor-beta-stimulated extracellular matrix production. *J Biol Chem*. 2013;288:14584-14598.
6. Van Duyn Graham L, Sweetwyne MT, Pallero MA, Murphy-Ullrich JE. Intracellular calreticulin regulates multiple steps in fibrillar collagen expression, trafficking, and processing into the extracellular matrix. *J Biol Chem*. 2010;285:7067-7078.
7. Owusu BY, Zimmerman KA, Murphy-Ullrich JE. The role of the endoplasmic reticulum protein calreticulin in mediating TGF-beta-stimulated extracellular matrix production in fibrotic disease. *J Cell Commun Signal*. 2018;12:289-299.
8. Groenendyk J, Lee D, Jung J, et al. Inhibition of the unfolded protein response mechanism prevents cardiac fibrosis. *PLoS One*. 2016;11:e0159682.
9. Groenendyk J, Robinson A, Wang Q, et al. Tauroursodeoxycholic acid attenuates cyclosporine-induced renal fibrogenesis in the mouse model. *Biochim Biophys Acta*. 2019;1863:1210-1216.

10. Peters LR, Raghavan M. Endoplasmic reticulum calcium depletion impacts chaperone secretion, innate immunity, and phagocytic uptake of cells. *J Immunol*. 2011;187:919-931.

11. Raghavan M, Del Cid N, Rizvi SM, Peters LR. MHC class I assembly: out and about. *Trends Immunol*. 2008;29:436-443.

12. Raghavan M, Wijeyesakere SJ, Peters LR, Del Cid N. Calreticulin in the immune system: ins and outs. *Trends Immunol*. 2013;34:13-21.

13. Honore C, Hummelshoj T, Hansen BE, Madsen HO, Eggleton P, Garred P. The innate immune component ficolin 3 (Hakata antigen) mediates the clearance of late apoptotic cells. *Arthritis Rheum*. 2007;56:1598-1607.

14. Apetoh L, Obeid M, Tesniere A, et al. Immunogenic chemotherapy: discovery of a critical protein through proteomic analyses of tumor cells. *Cancer Genomics Proteomics*. 2007;4:65-70.

15. Garg AD, Galluzzi L, Apetoh L, et al. Molecular and translational classifications of DAMPs in immunogenic cell death. *Front Immunol*. 2015;6:588.

16. Kepp O, Tesniere A, Zitvogel L, Kroemer G. The immunogenicity of tumor cell death. *Curr Opin Oncol*. 2009;21:71-76.

17. Obeid M, Panaretakis T, Joza N, et al. Calreticulin exposure is required for the immunogenicity of gamma-irradiation and UVC light-induced apoptosis. *Cell Death Differ*. 2007;14:1848-1850.

18. Obeid M, Panaretakis T, Tesniere A, et al. Leveraging the immune system during chemotherapy: moving calreticulin to the cell surface converts apoptotic death from "silent" to immunogenic. *Cancer Res*. 2007;67:7941-7944.

19. Obeid M, Tesniere A, Panaretakis T, et al. Ecto-calreticulin in immunogenic chemotherapy. *Immunol Rev*. 2007;220:22-34.

20. Tesniere A, Apetoh L, Ghiringhelli F, et al. Immunogenic cancer cell death: a key-lock paradigm. *Curr Opin Immunol*. 2008;20:504-511.

21. Gold LI, Pavlides SC, Ojeda J, Eaton B, Panchal RG. A new role for the multifunctional wound healing agent calreticulin in combating infection: significan for treating diabetic foot ulcers. *Wound Repair Regen*. 2014;22 (abstract oral presentation):A42.

22. Greives MR, Samra F, Pavlides SC, et al. Exogenous calreticulin improves diabetic wound healing. *Wound Repair Regen*. 2012;20:715-730.

23. Nanney LB, Woodrell CD, Greives MR, et al. Calreticulin enhances porcine wound repair by diverse biological effects. *Am J Pathol*. 2008;173:610-630.

24. Pandya UM, Gold LI. The novel biotherapeutic calreticulin (CRT) corrects multiple defects of non-healing diabetic wounds. *J Derm Clin Res*. 2016;4:1083-1093.

25. Huang ES, Basu A, O'Grady M, Capretta JC. Projecting the future diabetes population size and related costs for the U.S. *Diabetes Care*. 2009;32:2225-2229.

26. Clark RA, Ghosh K, Tonnesen MG. Tissue engineering for cutaneous wounds. *J Invest Dermatol*. 2007;127:1018-1029.

27. Zielins ER, Brett EA, Luan A, et al. Emerging drugs for the treatment of wound healing. *Expert Opin Emerg Drugs*. 2015;20:235-246.

28. Leavitt T, Hu MS, Marshall CD, Barnes LA, Lorenz HP, Longaker MT. Scarless wound healing: finding the right cells and signals. *Cell Tissue Res*. 2016;365:483-493.

29. Liu ZJ, Velazquez OC. Hyperoxia, endothelial progenitor cell mobilization, and diabetic wound healing. *Antioxid Redox Signal*. 2008;10:1869-1882.

30. Brem H, Sheehan P, Rosenberg HJ, Schneider JS, Boulton AJ. Evidence-based protocol for diabetic foot ulcers. *Plast Reconstr Surg*. 2006;117:193S-209S; discussion 210S-211S.

31. Elton CM, Smethurst PA, Eggleton P, Farndale RW. Physical and functional interaction between cell-surface calreticulin and the collagen receptors integrin alpha2beta1 and glycoprotein VI in human platelets. *Thromb Haemost*. 2002;88:648-654.

32. Gurtner GC, Werner S, Barrandon Y, Longaker MT. Wound repair and regeneration. *Nature*. 2008;453:314-321.

33. Barrientos S, Stojadinovic O, Golinko MS, Brem H, Tomic-Canic M. Growth factors and cytokines in wound healing. *Wound Repair Regen*. 2008;16:585-601.

34. Gardai SJ, McPhillips KA, Frasch SC, et al. Cell-surface calreticulin initiates clearance of viable or apoptotic cells through trans-activation of LRP on the phagocyte. *Cell*. 2005;123:321-334.

35. Gardai SJ, Xiao YQ, Dickinson M, et al. By binding SIRPalpha or calreticulin/CD91, lung collectins act as dual function surveillance molecules to suppress or enhance inflammation. *Cell*. 2003;115:13-23.

36. Huang SH, Zhao LX, Hong C, et al. Self-oligomerization is essential for enhanced immunological activities of soluble recombinant calreticulin. *PLoS One*. 2013;8:e64951.

37. Verrecchia F, Mauviel A. Transforming growth factor-beta and fibrosis. *World J Gastroenterol*. 2007;13:3056-3062.

38. Mori Y, Chen SJ, Varga J. Expression and regulation of intracellular SMAD signaling in scleroderma skin fibroblasts. *Arthritis Rheum*. 2003;48:1964-1978.

39. Strieter RM, Mehrad B. New mechanisms of pulmonary fibrosis. *Chest*. 2009;136:1364-1370.

40. Kim KK, Sheppard D, Chapman HA. TGF-beta1 signaling and tissue fibrosis. *Cold Spring Harb Perspect Biol*. 2018;10.

41. Khalil N, Parekh TV, O'Connor R, et al. Regulation of the effects of TGF-beta 1 by activation of latent TGF-beta 1 and differential expression of TGF-beta receptors (T beta R-I and T beta R-II) in idiopathic pulmonary fibrosis. *Thorax*. 2001;56:907-915.

42. Yamamoto T, Noble NA, Cohen AH, et al. Expression of transforming growth factor-beta isoforms in human glomerular diseases. *Kidney Int*. 1996;49:461-469.

43. Leask A. Focal adhesion kinase: a key mediator of transforming growth factor beta signaling in fibroblasts. *Adv Wound Care*. 2013;2:247-249.

44. Peidl A, Perbal B, Leask A. Yin/Yang expression of CCN family members: transforming growth factor beta 1, via ALK5/FAK/MEK, induces CCN1 and CCN2, yet suppresses CCN3, expression in human dermal fibroblasts. *PLoS One*. 2019;14:e0218178.

45. Massague J. TGFbeta signalling in context. *Nat Rev Mol Cell Biol*. 2012;13:616-630.

46. Ikushima H, Miyazono K. Biology of transforming growth factor-beta signaling. *Curr Pharm Biotechnol*. 2011;12:2099-2107.

47. Heldin CH, Moustakas A. Signaling receptors for TGF-beta family members. *Cold Spring Harb Perspect Biol*. 2016;8.

48. Morikawa M, Derynck R, Miyazono K. TGF-beta and the TGF-beta family: context-dependent roles in cell and tissue physiology. *Cold Spring Harb Perspect Biol*. 2016;8.

49. Kypreou KP, Kavvadas P, Karamessinis P, et al. Altered expression of calreticulin during the development of fibrosis. *Proteomics*. 2008;8:2407-2419.

50. Baksh S, Burns K, Busaan J, Michalak M. Expression and purification of recombinant and native calreticulin. *Protein Expr Purif*. 1992;3:322-331.

51. Galiano RD, Michaels J, Dobryansky M, Levine JP, Gurtner GC. Quantitative and reproducible murine model of excisional wound healing. *Wound Repair Regen*. 2004;12:485-492.

52. Pelton RW, Saxena B, Jones M, Moses HL, Gold LI. Immunohistochemical localization of TGF beta 1, TGF beta 2, and TGF beta 3 in the mouse embryo: expression patterns suggest multiple roles during embryonic development. *J Cell Biol*. 1991;115:1091-1105.

53. Arias JI, Parra N, Beato C, et al. Different Trypanosoma cruzi calreticulin domains mediate migration and proliferation of fibroblasts in vitro and skin wound healing in vivo. *Arch Dermatol Res*. 2018;310:639-650.

54. Gooch JL, Gorin Y, Zhang BX, Abboud HE. Involvement of calcineurin in transforming growth factor-beta-mediated regulation of extracellular matrix accumulation. *J Biol Chem*. 2004;279:15561-15570.

55. Derynck R, Zhang YE. Smad-dependent and Smad-independent pathways in TGF-beta family signalling. *Nature*. 2003;425:577-584.

56. Roberts AB. Molecular and cell biology of TGF-beta. *Miner Electrolyte Metab*. 1998;24:111-119.

57. Distler JHW, Gyorfi AH, Ramanujam M, Whitfield ML, Konigshoff M, Lafyatis R. Shared and distinct mechanisms of fibrosis. *Nat Rev Rheumatol*. 2019;15(12):705-730.

58. Martinovic Kaliterna D, Petric M. Biomarkers of skin and lung fibrosis in systemic sclerosis. *Exp Rev Clin Immunol*. 2019;15:1215-1223.

59. Khalil N, Parekh TV, O'Connor RN, Gold LI. Differential expression of transforming growth factor-beta type I and II receptors by pulmonary cells in bleomycin-induced lung injury: correlation with repair and fibrosis. *Exp Lung Res*. 2002;28:233-250.

60. Mori S, Kodaira M, Ito A, et al. Enhanced expression of integrin alphavbeta3 induced by TGF-beta is required for the enhancing effect of fibroblast growth factor 1 (FGF1) in TGF-beta-induced epithelial-mesenchymal transition (EMT) in mammary epithelial cells. *PLoS One*. 2015;10:e0137486.

61. Massague J, Heino J, Laiho M. Mechanisms in TGF-beta action. *Ciba Found Symp*. 1991;157:51-59; discussion 59-65.

62. Murphy-Ullrich JE. The de-adhesive activity of matricellular proteins: is intermediate cell adhesion an adaptive state? *J Clin Invest*. 2001;107:785-790.

63. Orr AW, Elzie CA, Kucik DF, Murphy-Ullrich JE. Thrombospondin signaling through the calreticulin/LDL receptor-related protein co-complex stimulates random and directed cell migration. *J Cell Sci*. 2003;116:2917-2927.

64. Orr AW, Pedraza CE, Pallero MA, et al. Low density lipoprotein receptor-related protein is a calreticulin coreceptor that signals focal adhesion disassembly. *J Cell Biol*. 2003;161:1179-1189.

65. Lillis AP, Van Duyn LB, Murphy-Ullrich JE, Strickland DK. LDL receptor-related protein 1: unique tissue-specific functions revealed by selective gene knockout studies. *Physiol Rev*. 2008;88:887-918.

66. Obermoeller LM, Warshawsky I, Wardell MR, Bu G. Differential functions of triplicated repeats suggest two independent roles for the receptor-associated protein as a molecular chaperone. *J Biol Chem*. 1997;272:10761-10768.

67. Fadel MP, Szewczenko-Pawlikowski M, Leclerc P, et al. Calreticulin affects beta-catenin-associated pathways. *J Biol Chem*. 2001;276:27083-27089.

68. Gold LI, Rahman M, Blechman KM, et al. Overview of the role for calreticulin in the enhancement of wound healing through multiple biological effects. *J Investig Dermatol Symp Proc*. 2006;11:57-65.

69. Verrecchia F, Mauviel A, Farge D. Transforming growth factor-beta signaling through the Smad proteins: role in systemic sclerosis. *Autoimmun Rev*. 2006;5:563-569.

70. Verrecchia F, Laboureau J, Verola O, et al. Skin involvement in scleroderma—where histological and clinical scores meet. *Rheumatology (Oxford)*. 2007;46:833-841.

71. Flanders KC, Sullivan CD, Fujii M, et al. Mice lacking Smad3 are protected against cutaneous injury induced by ionizing radiation. *Am J Pathol*. 2002;160:1057-1068.

72. Sweetwyne MT, Pallero MA, Lu A, Van Duyn Graham L, Murphy-Ullrich JE. The calreticulin-binding sequence of thrombospondin 1 regulates collagen expression and organization during tissue remodeling. *Am J Pathol*. 2010;177:1710-1724.

73. Schnittert J, Bansal R, Storm G, Prakash J. Integrins in wound healing, fibrosis and tumor stroma: high potential targets for therapeutics and drug delivery. *Adv Drug Deliv Rev*. 2018;129:37-53.

74. Clark RA, Tonnesen MG, Gailit J, Cheresh DA. Transient functional expression of alphaVbeta 3 on vascular cells during wound repair. *Am J Pathol*. 1996;148:1407-1421.

75. Kubo M, Van de Water L, Plantefaber LC, et al. Fibrinogen and fibrin are anti-adhesive for keratinocytes: a mechanism for fibrin eschar slough during wound repair. *J Invest Dermatol*. 2001;117:1369-1381.

76. McDonald JA, Kelley DG, Broekelmann TJ. Role of fibronectin in collagen deposition: Fab' to the gelatin-binding domain of fibronectin inhibits both fibronectin and collagen organization in fibroblast extracellular matrix. *J Cell Biol*. 1982;92:485-492.

77. Sottile J, Hocking DC. Fibronectin polymerization regulates the composition and stability of extracellular matrix fibrils and cell-matrix adhesions. *Mol Biol Cell*. 2002;13:3546-3559.

78. Leiss M, Beckmann K, Giros A, Costell M, Fassler R. The role of integrin binding sites in fibronectin matrix assembly in vivo. *Curr Opin Cell Biol*. 2008;20:502-507.

79. Chantre CO, Campbell PH, Golecki HM, et al. Production-scale fibronectin nanofibers promote wound closure and tissue repair in a dermal mouse model. *Biomaterials*. 2018;166:96-108.

80. Bandyopadhyay B, Fan J, Guan S, et al. A "traffic control" role for TGFbeta3: orchestrating dermal and epidermal cell motility during wound healing. *J Cell Biol*. 2006;172:1093-1105.

81. Flanders KC, Holder MG, Winokur TS. Autoinduction of mRNA and protein expression for transforming growth factor-beta S in cultured cardiac cells. *J Mol Cell Cardiol*. 1995;27:805-812.

82. Wordinger RJ, Sharma T, Clark AF. The role of TGF-β2 and bone morphogenetic proteins in the trabecular meshwork and glaucoma. *J Ocul Pharmacol Ther*. 2014;30:154-162.

83. Walton KL, Johnson KE, Harrison CA. Targeting TGF-β mediated SMAD signaling for the prevention of fibrosis. *Front Pharmacol*. 2017;8:461.

84. Occleston NL, Fairlamb D, Hutchison J, O'Kane S, Ferguson MW. Avotermin for the improvement of scar appearance: a new pharmaceutical in a new therapeutic area. *Expert Opin Investig Drugs*. 2009;18:1231-1239.

85. Goicoechea S, Orr AW, Pallero MA, Eggleton P, Murphy-Ullrich JE. Thrombospondin mediates focal adhesion disassembly through interactions with cell surface calreticulin. *J Biol Chem*. 2000;275:36358-36368.

86. Herz J, Strickland DK. LRP: a multifunctional scavenger and signaling receptor. *J Clin Invest*. 2001;108:779-784.

87. Lee D, Walsh JD, Migliorini M, et al. The structure of receptor-associated protein (RAP). *Protein Sci*. 2007;16:1628-1640.

88. Huang SS, Huang JS. TGF-beta control of cell proliferation. *J Cell Biochem*. 2005;96:447-462.

89. Tseng WF, Huang SS, Huang JS. LRP-1/TbetaR-V mediates TGF-beta1-induced growth inhibition in CHO cells. *FEBS Lett*. 2004;562:71-78.

90. He MC, Wang J, Wu J, et al. Immunological activity difference between native calreticulin monomers and oligomers. *PLoS One*. 2014;9:e105502.

91. Duo CC, Gong FY, He XY, et al. Soluble calreticulin induces tumor necrosis factor-alpha (TNF-alpha) and interleukin (IL)-6 production by macrophages through mitogen-activated protein kinase (MAPK) and NFkappaB signaling pathways. *Int J Mol Sci*. 2014;15:2916-2928.

92. Rauch F, Prud'homme J, Arabian A, Dedhar S, St-Arnaud R. Heart, brain, and body wall defects in mice lacking calreticulin. *Exp Cell Res*. 2000;256:105-111.

93. Papp S, Fadel MP, Kim H, McCulloch CA, Opas M. Calreticulin affects fibronectin-based cell-substratum adhesion via the regulation of c-Src activity. *J Biol Chem*. 2007;282:16585-16598.

94. Papp S, Szabo E, Kim H, McCulloch CA, Opas M. Kinase-dependent adhesion to fibronectin: regulation by calreticulin. *Exp Cell Res*. 2008;314:1313-1326.

95. Wu M, Massaeli H, Durston M, Mesaeli N. Differential expression and activity of matrix metalloproteinase-2 and -9 in the calreticulin deficient cells. *Matrix Biol*. 2007;26:463-472.

96. Coppolino MG, Woodside MJ, Demaurex N, Grinstein S, St-Arnaud R, Dedhar S. Calreticulin is essential for integrin-mediated calcium signalling and cell adhesion. *Nature*. 1997;386:843-847.

97. Kwon MS, Park CS, Choi K-R, et al. Calreticulin couples calcium release and calcium influx in integrin-mediated calcium signaling. *Mol Biol Cell*. 2000;11:1433-1443.

98. Ruseska I, Zimmer A. Internalization mechanisms of cell-penetrating peptides. *Beilstein J. Nanotechnol*. 2020;11:101-123.

99. Barker TH, Grenett HE, MacEwen MW, et al. Thy-1 regulates fibroblast focal adhesions, cytoskeletal organization and migration through modulation of p190 RhoGAP and Rho GTPase activity. *Exp Cell Res*. 2004;295:488-496.

100. Orr AW, Pallero MA, Xiong WC, Murphy-Ullrich JE. Thrombospondin induces RhoA inactivation through FAK-dependent signaling to stimulate focal adhesion disassembly. *J Biol Chem*. 2004;279:48983-48992.

101. Karimzadeh F, Opas M. Calreticulin is required for TGF-beta-induced epithelial-to-mesenchymal transition during cardiogenesis in mouse embryonic stem cells. *Stem Cell Rep*. 2017;8:1299-1311.

102. Zimmerman KA, Xing D, Pallero MA, et al. Calreticulin regulates neointima formation and collagen deposition following carotid artery ligation. *J Vasc Res*. 2016;52:306-320.

103. Goicoechea S, Pallero MA, Eggleton P, Michalak M, Murphy-Ullrich JE. The anti-adhesive activity of thrombospondin is mediated by the N-terminal domain of cell surface calreticulin. *J Biol Chem*. 2002;277:37219-37228.

SUPPORTING INFORMATION

Additional supporting information may be found online in the Supporting Information section.